Partner-specific induction of Spodoptera frugiperda immune genes in response to the entomopathogenic nematobacterial complex Steinernema carpocapsae-Xenorhabdus nematophila

Louise Huot, Audrey Bigourdan, Sylvie Pages, Jean-Claude Ogier, Pierre-Alain Girard, Nicolas Nègre, Bernard Duvic

▶ **To cite this version:**

Louise Huot, Audrey Bigourdan, Sylvie Pages, Jean-Claude Ogier, Pierre-Alain Girard, et al.. Partner-specific induction of Spodoptera frugiperda immune genes in response to the entomopathogenic nematobacterial complex Steinernema carpocapsae-Xenorhabdus nematophila. Developmental and Comparative Immunology, 2020, 108, 10.1016/j.dci.2020.103676 . hal-02516411

HAL Id: hal-02516411
https://hal.inrae.fr/hal-02516411

Submitted on 20 May 2022

HAL is a multi-disciplinary open access archive for the deposit and dissemination of scientific research documents, whether they are published or not. The documents may come from teaching and research institutions in France or abroad, or from public or private research centers.

L'archive ouverte pluridisciplinaire **HAL**, est destinée au dépôt et à la diffusion de documents scientifiques de niveau recherche, publiés ou non, émanant des établissements d'enseignement et de recherche français ou étrangers, des laboratoires publics ou privés.

Distributed under a Creative Commons Attribution - NonCommercial 4.0 International License

Version of Record: https://www.sciencedirect.com/science/article/pii/S0145305X20300409
Manuscript_c72c270486634b4999aad3045b11658d

Partner-specific induction of *Spodoptera frugiperda* immune genes in response to the entomopathogenic nematobacterial complex *Steinernema carpocapsae-Xenorhabdus nematophila*

Louise Huot[1], Audrey Bigourdan[1], Sylvie Pagès[1], Jean-Claude Ogier[1], Pierre-Alain Girard[1], Nicolas Nègre[1,*] and Bernard Duvic[1,*]

[1] DGIMI, Univ Montpellier, INRAE, Montpellier, France

[*] Co-corresponding authors

E-mail: nicolas.negre@umontpellier.fr (NN) ; bernard.duvic@umontpellier.fr (BD)

© 2020 published by Elsevier. This manuscript is made available under the CC BY NC user license
https://creativecommons.org/licenses/by-nc/4.0/

Abstract

The *Steinernema carpocapsae-Xenorhabdus nematophila* association is a nematobacterial complex used in biological control of insect crop pests. The infection success of this dual pathogen strongly depends on its interactions with the host's immune system. Here, we used the lepidopteran pest *Spodoptera frugiperda* to analyze the respective impact of each partner in the induction of its immune responses. First, we used previously obtained RNAseq data to construct the immunome of *S. frugiperda* and analyze its induction. We then selected representative genes to study by RT-qPCR their induction kinetics and specificity after independent injections of each partner. We showed that both *X. nematophila* and *S. carpocapsae* participate in the induction of stable immune responses to the complex. While *X. nematophila* mainly induces genes classically involved in antibacterial responses, *S. carpocapsae* induces lectins and genes involved in melanization and encapsulation. We discuss putative relationships between these differential inductions and the pathogen immunosuppressive strategies.

Keywords

Steinernema carpocapsae, *Xenorhabdus nematophila*, *Spodoptera frugiperda*, nematobacterial complex, immunome, transcriptional response

Abbreviations[1]

1. Introduction

The *Steinernema-Xenorhabdus* nematobacterial complexes (NBCs) are natural symbiotic associations between nematodes and enterobacteria that are pathogenic for insects. The soil-living nematodes infest insects through the respiratory and/or the intestinal tract (Dowds and Peters, 2002) and reach the hemocoel, the internal body cavity, where they release their intestinal symbionts. The bacteria then grow extracellularly in the hemolymph, the insect equivalent of blood, and improve the nematodes' pathogenicity as well as their ability to reproduce in the host dead body (Forst and Clarke, 2002). Until now, about 90 species of *Steinernema* have been identified, among which several are usable as biological control agents against diverse insect crop pests (Labaude and Griffin, 2018; Lacey et al., 2015). In consequence, their interactions with insects have been extensively studied for about 50 years (Poinar and Grewal, 2012). These studies have shown that in addition to ecological and morphological parameters (Labaude and Griffin, 2018), the NBCs' interactions with the host's immune system is one of the most

[1] NBC: nematobacterial complex; AMP: antimicrobial peptides; NBTA: Nutrient bromothymol blue agar; PBS: phosphate buffered saline; CFU: Colony-forming unit; GNBP: Gram-negative binding protein; PGRP: Peptidoglycan recognition protein; LLP: Lysozyme-like protein; PPAE: Prophenoloxidase-activating enzyme; IMPI: Insect metalloproteinase inhibitor protein; TEP: Tiol-ester protein

crucial factors influencing their ability to infest and kill a given insect (Li et al., 2007; Thurston et al., 1994; Wang et al., 1994).

Insects possess an elaborate immune system, which is able to respond appropriately to diverse types of pathogens and of infections. Firstly, this system involves protective external barriers such as the cuticle, or the peritrophic matrix in the midgut (Kristensen and Chauvin, 2012; Lehane, 1997). It then relies on local defenses of the surface epithelia, which repair efficiently (Ferrandon, 2013; Galko and Krasnow, 2004; Rowley and Ratcliffe, 1978) and produce toxic factors such as antimicrobial peptides (AMPs) (Brey et al., 1993; Tingvall et al., 2001; Tzou et al., 2000; Wu et al., 2010) and reactive oxygen species (Ha et al., 2009). The third line of defense of insects is provided by the hemocytes, which are the circulating immune cells. They can produce diverse types of immune responses, including AMP synthesis, phagocytosis, nodulation, encapsulation, coagulation and melanization (Strand, 2008). Nodulation and encapsulation are cellular immune responses respectively consisting in the engulfment of bacterial aggregates and of large invaders via hemocytes aggregation (Strand, 2008). Together with coagulation, these responses are coupled with a melanization process consisting of series of phenolic compounds oxidations resulting in synthesis of reactive molecules and melanin that participate in pathogens trapping and killing (Jiravanichpaisal et al., 2006; Nappi and Christensen, 2005). Finally, the fat body, a functional equivalent of the mammalian liver, produces potent systemic humoral immune responses involving a massive secretion of AMP cocktails in the hemolymph. These responses can be induced by two major signaling pathways of insect immunity; the Imd pathway, which is mainly activated by Gram negative bacteria, and/or the Toll pathway, which is mainly activated by Gram positive bacteria, fungal organisms and by proteases released by pathogens (Ferrandon et al., 2007; Issa et al., 2018).

The *Steinernema-Xenorhabdus* NBC whose interactions with the immune system have been the most extensively studied is the *S. carpocapsae-X. nematophila* association. These interactions have firstly been studied from the NBC point of view, which allowed the identification of a multitude of immunoevasive and immunosuppressive strategies. For instance, studies in *Rhynchophorus ferrugineus* and *Galleria mellonella* have respectively shown that the cuticle of *S. carpocapsae* is not recognized by the host's immune system (Binda-Rossetti et al., 2016; Mastore et al., 2015) and that the nematode secretes protease inhibitors impairing the coagulation responses (Toubarro et al., 2013a; Toubarro et al., 2013b). Studies in diverse insect models have also shown that both partners produce factors impairing melanization (Balasubramanian et al., 2009; Balasubramanian et al., 2010; Crawford et al., 2012; Eom et al., 2014), hemocyte's viability (Brivio et al., 2018; Kim et al., 2005; Ribeiro et al., 1999; Ribeiro et al., 2003; Vigneux et al., 2007) and the production of cellular immune responses by several ways (Balasubramanian et al., 2009; Balasubramanian et al., 2010; Eom et al., 2014; Park and Kim, 2000; Park and Stanley, 2006; Toubarro et al., 2013b). Finally, both *X. nematophila* and *S. carpocapsae* secrete proteolytic factors

degrading cecropin AMPs (Caldas et al., 2002; Gotz et al., 1981) and the bacterium has also been shown to reduce more globally the hemolymph antimicrobial activity, as well as AMP transcription in lepidopteran models (Binda-Rossetti et al., 2016; Caldas et al., 2002; Duvic et al., 2012; Ji and Kim, 2004).

On the other hand, the description of these interactions from the hosts' points of view is at its beginning. This aspect has mainly been studied in the *Drosophila melanogaster* model, with a first transcriptomic analysis of the whole larva responses to infestations by entire NBCs and by axenic nematodes (Yadav et al., 2017). This analysis has shown that several immune processes are induced by both pathogens at the transcriptional level. For instance, the authors found in each case an overexpression of genes related to the Imd and Toll pathways that was accompanied by the induction of a few AMP genes. They also found an upregulation of genes related to melanization, coagulation, or involved in the regulation of cellular immune responses (Yadav et al., 2017). Complementary gene knockout experiments in this model demonstrated an involvement of the Imd pathway in the response against *X. nematophila* (Aymeric et al., 2010) and revealed a possible involvement of the Imaginal Disc Growth Factor-2, the intestinal serine protease Jonah 66Ci (Yadav and Eleftherianos, 2019) as well as TGF-β and JNK pathways members in the regulation of anti-nematode immunity (Yadav and Eleftherianos, 2018; Yadav et al., 2018).

In order to improve our understanding of the dialogue that takes place between this NBC and its host, we recently published a topologic transcriptomic analysis of the response of the lepidopteran model *Spodoptera frugiperda* to the infestation (Huot et al., 2019). This analysis was focused on the three main immunocompetent tissues that are confronted to the NBC, which are the midgut (the main entry site in the hemocoel), the hemocytes and the fat body. The RNAseq experiment showed that there was no potent or well-defined transcriptional response in the midgut. However, we observed dramatic transcriptional responses in the fat body and the hemocytes at 15 h post-infestation, which is a middle time point of the infection. In agreement with the results obtained in *D. melanogaster* whole larvae (Yadav et al., 2017), global analysis of these responses showed they are dominated by immune processes. The objective of the present study is to go further in the analysis of these induced immune responses. In order to describe them with high accuracy, we first examine the expression variations of all the immune genes that have been identified in the insect's genome. We then use tissue RT-qPCR experiments to analyze the temporal dynamics and the relative contribution of each NBC partner in the identified immune responses. Our results show that a large number of immune genes are responsive in either one or the two tissues during the infestation, with activation of antimicrobial and cellular immunities, of melanization, coagulation and of metalloprotease inhibition. These responses were found to be stable over the time post-infestation and to consist in combinations of *X. nematophila*-induced and *S. carpocapsae*-induced responses in each tissue. The *X. nematophila*-induced responses mainly correspond to genes that are classically involved in antibacterial immunity, whereas the *S. carpocapsae*-induced ones mainly include lectins and genes

potentially involved in melanization and encapsulation. In addition, our RT-qPCR experiments show that two previously identified candidate clusters of uncharacterized genes (Huot et al., 2019) also present partner-specific induction profiles. Our hypothesis is that they may correspond to new types of anti-nematode and antibacterial immune factors found in *Spodoptera* genus and lepidopteran species, respectively.

2. Materials and Methods

2.1. Insect rearing

Corn-strain *Spodoptera frugiperda* (Lepidoptera : Noctuidae) were fed on corn-based artificial diet (Poitout and Buès, 1970). They were reared at 23°C +/- 1°C with a photoperiod of 16 h/8 h (light/dark) and a relative humidity of 40 % +/- 5 %. *Galleria mellonella* (Lepidoptera : Pyralidae) were reared on honey and pollen at 28°C in dark.

2.2. Production and storage of nematobacterial complexes

Steinernema carpocapsae-Xenorhabdus nematophila complexes (strain SK27 isolated from Plougastel, France) were renewed by infestation of one month-old *Galleria mellonella* larvae. They were collected on White traps (White, 1927) and stored at 8°C in aerated Ringer sterile solution with 0.1 % formaldehyde. The maximal time of storage was limited to 4 weeks to avoid pathogenicity losses.

2.3. Production of axenic nematodes

Gravid *S. carpocapsae* females were extracted from *G. mellonella* dead bodies at day 4 to 6 after infestation by nematobacterial complexes (NBCs). After 5 washing steps in Ringer sterile solution, the females were surface-sterilized by 20 min incubation in 0.48 % (wt/vol) sodium hypochlorite and 3 h incubation in Ringer sterile solution supplemented with antibiotics (150 µg/mL polymyxin, 50 µg/mL colistin, 50 µg/mL nalidixic acid). The eggs were extracted by female crushing with sterile glass pestles and then washed by centrifugation (2 min, 16000 g) in Ringer sterile solution, disinfected by incubation in 0.48 % sodium hypochlorite for 5 min, and washed again twice. After microscopic observation, the intact eggs were placed on liver-agar (40 g/L Tryptycase Soja Agar [BioMérieux], 5 g/L Yeast Extract [Difco], 100 g/L porc liver) plates supplemented with antibiotics (150 µg/mL polymyxin, 50 µg/mL colistin and 50 µg/mL nalidixic acid). The plates were maintained inside a dark humid chamber for 1 month to allow nematodes development. The nematodes were then suspended in Ringer sterile solution and infective juvenile stages (IJs) were sorted by pipetting under a microscope (Leica). The IJs were rinsed twice by centrifugation (2 min, 3000 g) in 1 mL Ringer sterile solution and used within minutes for experimental infection.

Nematodes' axenicity was verified by DNA extraction and PCR amplification. Nematodes were suspended in 200 µL milliQ water supplemented with 200 µL glass beads (Ø ⩽ 106 µm) (Sigma). They were ground for 2 x 40 sec at 4.5 ms speed with a FastPrep homogenizer (MP Biomedicals). The debris were discarded by centrifugation (2 min, 16000 g) and 150 µL supernatant were mixed with 200 µL lysis buffer (Quick extract kit, Epi-centre) for a second grinding. To ensure bacterial cell lysis, the samples were incubated at room temperature for 48 h with 2 µL Ready-Lyse Lysozyme solution at 30000 U/µL (Epi-centre). Protein denaturation was then performed by 10 min incubation at 90°C, and RNA was removed by 10 min incubation at 37°C with 20 µL RNase A (20 mg/mL) (Invitrogen). DNA was extracted by successive addition of 500 µL phenol-chloroform-isoamyl alcohol and 500 µL chloroform, followed by centrifugations (10 min, 16000 g) and aqueous phase collections. DNA was precipitated with 500 µL 100% ethanol supplemented with 20 µL sodium acetate and by freezing at -80°C for 2 h. After defrosting, DNA was concentrated by centrifugation (30 min, 16000 g) and the precipitates were washed twice by centrifugation (15 min, 16000 g) in 500 µL 70% ethanol. DNA was finally suspended in 50 µL sterile milliQ water and left at room temperature for a few hours to ensure precipitate dissolution. After DNA quantification with a Qubit fluorometer (Invitrogen), *X. nematophila* presence was assessed by PCR amplification with *Xenorhabdus*-specific primers (Xeno_F: 5'-ATG GCG CCA ATA ACC GCA ACT A-3'; Xeno_R: 5'-TGG TTT CCA CTT TGG TAT TGA TGC C-3'), which target a region of the XNC1_0073 gene encoding a putative TonB-dependent heme-receptor (Cambon et al., 2020). The presence of other bacteria was assessed by 16S rRNA gene amplification with universal primers (Tailliez et al., 2006). Thirty cycles of PCR were performed using Taq polymerase (Invitrogen) in a Biorad thermocycler, with hybridization temperatures of 55°C and 50°C respectively. PCR products were then analyzed by agarose gel electrophoresis with DNAs from *X. nematophila*, *Pseudomonas protegens* and *S. carpocapsae-X. nematophila* complexes as controls (Supplementary Fig. 1).

2.4. Experimental infections

Experimental infestations with NBCs were carried out on individual 2nd day 6th instar *S. frugiperda* larvae according to Huot et al. (2019). Briefly, 12-well plates were coated with pieces of filter paper (Whatman) and larvae were individually introduced in each well with a cube of artificial diet (Poitout and Buès, 1970). For infestations, 150 +/- 20 NBCs in 150 µL Ringer sterile solution were poured in each well and the plates were then maintained at 23°C. 150 µL Ringer sterile solution were used for control experiments.

For intra-hemocoelic injection experiments, pathogens were injected in larvae's abdomens after local application of 70% ethanol with a paintbrush. Injections were performed using a syringe pump (Delta labo) with 1 mL syringes (Terumo) and 25G needles (Terumo). The injected larvae were then kept in 12-well plates at 23 °C with cubes of artificial diet (Poitout and Buès, 1970).

X. nematophila suspensions were prepared as described in Sicard et al. (2004). Bacterial culture was diluted in PBS and 20 µL containing 200 +/- 50 bacterial cells were injected in the hemocoel at a rate of 1.67 mL/min. 20 µL sterile PBS were used for control larvae. The purity and number of injected *X. nematophila* were verified by plating 20 µL of the bacterial suspension on NBTA (Boemare et al., 1997).

For NBC and axenic nematode injections, 10 +/- 3 nematodes in 20 µL 70% Ringer and 30% glycerol solution were injected at a rate of 2.23 mL/min. Syringes were frequently renewed in order to limit nematodes concentration and sedimentation and the number of injected nematodes was verified by 10 simulations of injection in Petri dishes followed by nematode counting under a stereomicroscope (Zeiss). Sterile 70% Ringer and 30% glycerol solutions were used for control larvae. To avoid accidental *per os* infections, the injected larvae were then briefly washed in sterile PBS and dried on paper towel before being placed in 12-well plates.

The pathogens efficacies were checked by monitoring the survival of 12 control and 12 infected larvae for 72 h after infestation or after injection.

2.5. Production and storage of bacterial symbionts

X. nematophila strain F1 isolated from NBCs strain SK27 was conserved at -80°C. Within 3 weeks before each experiment, they were grown for 48 h at 28°C on NBTA supplemented with erythromycin (15 µg/mL) to which the strain is resistant (Sicard et al., 2004). The colonies were then conserved at 15°C and used for overnight culture at 28°C in 5 mL Luria-Bertani broth (LB) before experiments.

2.6. Caterpillar RNA extraction

RNAs were prepared as described in Huot et al. (2019). Briefly, nine larvae per technical replicate were bled in anti-coagulant buffer (van Sambeek and Wiesner, 1999). Hemocytes were recovered by centrifugation (1 min, 800 g) at 4°C and the pellet was immediately flash-frozen with liquid nitrogen. The larvae were then dissected for fat body and midgut sampling and the tissues were flash-frozen in eppendorf tubes with liquid nitrogen. After storage at -80°C for at least 24 h, 1 mL Trizol (Life technologies) was added to the pooled tissues. The tissues were then ground by using a TissueLyzer 85210 Rotator (Qiagen) with one stainless steel bead (Ø : 3 mm) at 30 Hz for 3 min. For optimal cell lyses, ground tissues were left at room temperature for 5 min. To extract nucleic acids, 200 µL chloroform (Interchim) were added and the preparations were left at room temperature for 2 min with frequent vortex homogenization. After centrifugation (15 min, 15,000 g) at 4°C, the aqueous phases were transferred in new tubes and 400 µL 70% ethanol were added. RNA purifications were immediately performed with the RNeasy mini kit (Qiagen) and contaminant DNA was removed with the Turbo DNA-free™ kit (Life Technologies).

RNA yield and preparation purity were analyzed by measuring the ratios A_{260}/A_{280} and A_{260}/A_{230} with a Nanodrop 2000 spectrophotometer (Thermo Scientific). RNA integrity was verified by agarose gel electrophoresis and RNA preparations were conserved at - 80 °C.

2.7. RNAseq experiments

RNAseq raw data originate from Huot et al. (2019). In brief, during 3 independent experiments, 9 larvae infested with 150 *S. carpocapsae-X. nematophila* complexes and 9 uninfected control larvae were bled and dissected at time 15 hours post-contact with NBCs or Ringer sterile solution (see Materials and Methods 2.4.). Total RNA from their hemocytes and fat bodies were extracted (see Materials and Methods 2.6.) and the corresponding libraries were prepared by MGX GenomiX (IGF, Montpellier, France) with the TruSeq Stranded mRNA sample preparation kit (Illumina). The libraries were then validated on Fragment Analyzer with a Standard Sensitivity NGS kit (Advanced Analytical Technologies, Inc) and quantified by qPCR with a Light Cycler 480 thermal cycler (Roche Molecular diagnostics). cDNAs were then multiplexed by 6 and sequenced on 50 base pairs in a HiSeq 2500 system (Illumina) with a single-end protocol. Image analysis and base calling were performed with the HiSeq Control and the RTA software (Illumina). After demultiplexing, the sequences quality and the absence of contaminant were checked with the FastQC and the FastQ Screen softwares. Data were then submitted to a Purity Filter (Illumina) to remove overlapping clusters.

For each sample, the reads were pseudoaligned on the *S. frugiperda* reference transcriptome version OGS2.2 (Gouin et al., 2017) using the Kallisto software (Bray et al., 2016). Differential expression between infested and control conditions were then assessed for each time point and tissue with the Sleuth software (Pimentel et al., 2017). Wald tests were used with a q-value (equivalent of the adjusted p-value) threshold of 0.01 and a beta value (biased equivalent of the log2 fold change) threshold of 1. Only transcripts with normalized counts over 5 in all three replicates of the infested and/or of the control condition were considered as reliably differentially expressed.

Previously annotated immune transcripts (Gouin et al., 2017) were then checked for significant expression changes and not annotated differentially expressed ones were researched with the Blast2GO software by blastx on the NCBI nr and drosophila databases (Conesa et al., 2005). To avoid mistakes related to genome fragmentation, the immune transcripts were gathered by unique gene after careful examination of their sequences and of the available genomic data (Gouin et al., 2017). The induction levels of the transcripts were then averaged by unique gene before graphical representation of the results.

2.8. RT-qPCR experiments

RT-qPCR experiments were performed with extracted total RNA (see Materials and Methods 2.6.) from hemocytes and fat bodies of 9 larvae infested or infected by injection and of 9 uninfected control larvae during 3 independent experiments.

For each sample, cDNAs were synthesized from 1 µg of RNA with the SuperScript II Reverse Transcriptase (Invitrogen), according to the manufacturer's protocol.

The primers (Supplementary Table 1) were designed with the Primer3Web tool (Untergasser et al., 2012). Their efficiency was estimated by using serial dilutions of pooled cDNA samples and their specificity was verified with melting curves analyses. Amplification and melting curves were analyzed with the LightCycler 480 software (Roche Molecular diagnostics).

RT-qPCRs were carried out in technical triplicate, with the LightCycler 480 SYBR Green I Master kit (Roche). For each replicate and primer pair, 1.25 µL of sample containing 50 ng/µL of cDNA and 1.75 µL of Master mix containing 0.85 µM of primers were distributed in multiwell plates by an Echo 525 liquid handler (Labcyte). The amplification reactions were then performed in a LightCycler 480 thermal cycler (Roche) with an enzyme activation step of 15 min at 95°C, and 45 cycles of denaturation at 95°C for 5 sec, hybridization at 60°C for 10 sec and elongation at 72°C for 15 sec.

Crossing points were determined using the Second Derivative Maximum method with the LightCycler 480 software (Roche) and relative expression ratios between control and infected conditions were manually calculated according to the method of Ganger et al. (2017). The ratios were normalized to the RpL32 housekeeping gene relative levels and the EF1 gene was used as an internal control.

Statistical analyses of the data were all performed with the R software (R Core Team, 2017). Differential expression significance between the control and infected conditions was assessed by paired one-tailed t-tests on ΔCq values. Multiple comparisons of fold changes were assessed by one-way ANOVA on ΔΔCq values followed by post hoc Tukey tests. P-values under 0.05 were considered as significant for all the above tests. The gplots package was used to draw the heatmaps and the clusters were built from a dissimilarity matrix based on Pearson correlation coefficients.

2.9. Quantification of nematodes in the midgut lumen

NBCs in the midgut lumen were quantified at several times after infestation by nematode counting in the alimentary bolus. For 3 independent experiments, 3 infested larvae were dissected and the midguts' alimentary bolus were extracted. Each alimentary bolus was then dissolved in 3 mL sterile PBS in a Petri dish (Ø : 35 mm) and motile nematodes were counted with a stereomicroscope (Leica).

2.10. Quantification of *X. nematophila* in the hemolymph

The concentration of *X. nematophila* strain F1 in the hemolymph was estimated by CFU counting on selective medium. For 3 independent infestation or infection by injection experiments and 3 technical replicates, hemolymph was collected by bleeding of 3 caterpillars in 200 µL PBS supplemented with phenylthiourea (Sigma). The volumes of hemolymph were then estimated by pipetting and serial dilutions of the samples were plated on NBTA with 15 µg/mL erythromycin. CFU were counted after 48 h

incubation at 28°C and the counts were reported to the estimated hemolymph volumes in order to calculate the bacterial concentrations. Hemolymph of naive larvae was also plated for control.

2.11. Insect survival kinetics

Survival kinetics were measured by 3 independent experiments on pools of 20 larvae infested with NBCs or injected with NBCs, with axenic *S. carpocapsae* nematodes or with *X. nematophila* symbionts. Survival was monitored from 0 to 72 hours after contact or injection.

2.12. Parasitic success measurement

Parasitic success was measured during 3 independent experiments on pools of 20 NBCs or axenic nematodes-injected larvae. Dead larvae were individually placed on white traps (White, 1927) approximately 2 days after their deaths. The emergence of nematodes was assessed at day 40 after injection by observation of the collection liquid with a stereomicroscope (Leica). Parasitic success was then calculated as the percentage of larvae with nematode emergence among the infected larvae.

3. Results & Discussion

3.1. Hemocytes' and fat body's immune responses

In order to get an accurate picture of the *S. frugiperda* transcriptional immune responses to the NBC infestation, we first used a previously published list of immune genes identified by sequence homology in the *S. frugiperda* genome (Gouin et al., 2017). We then used previously obtained RNAseq data (Huot et al., 2019) to look at their expression variations in the fat body and in the hemocytes (Supplementary Table 2A) and we completed the repertoire with additional putative immune genes that we directly identified from lists of differentially expressed genes upon NBC infestation (Supplementary Table 2B). In total, we present the annotation of 226 immune or putative immune genes of which 132 were significantly modulated at 15 h post-infestation (hpi) (Sleuth, p-value < 0.01; |Beta| > 1; all count values > 5 in at least one condition) in one or both tissues (Fig. 1). Among them, 62 were involved in antimicrobial responses (Fig. 1A), 18 were related to melanization (Fig. 1B), 23 were involved in cellular responses (Fig. 1C) and the 29 remaining genes were grouped in a category called "diverse" due to pleiotropic or poorly characterized functions (Fig. 1D).

3.1.1. Antimicrobial responses

In the antimicrobial response category, 58 genes were found to be upregulated in at least one of the two tissues (Fig. 1A). The signaling genes encoded 3 and 8 members of the Imd and Toll pathways, respectively, as well as 5 short catalytic peptidoglycan recognition proteins (PGRP-S), which are probably involved in the regulation of these pathways by peptidoglycan degradation (Myllymaki et al., 2014; Valanne et al., 2011) (Fig. 1A). Four other genes were considered as involved in recognition. They

encoded Gram negative binding proteins (GNBPs), which have been reported to recognize peptidoglycans or β-glucans and participate in the further activation of the Toll pathway (Ferrandon et al., 2007) and/or of the melanization response (Nakhleh et al., 2017) (Fig. 1A). Finally, the effector genes encoded 33 antimicrobial peptides (AMPs) belonging to all the *S. frugiperda*'s AMP families (Gouin et al., 2017) plus 4 lysozymes and lysozyme-like proteins (LLPs) (Fig. 1A). Depending on their families and on the insect species, AMPs can present varied activity spectra, ranging from antiviral or antibacterial activities to anti-fungal and anti-parasitic ones (Yi et al., 2014). Varied activity spectra have also been found for several insects' lysozymes and LLPs (Chen et al., 2018; Gandhe et al., 2007; Satyavathi et al., 2018; Sowa-Jasilek et al., 2014; Yu et al., 2002). Interestingly, all of the categories and subcategories cited above were represented in the two tissues, indicating that their antimicrobial responses are diversified and that the factors responsible for their disappearance in the hemolymph (Binda-Rossetti et al., 2016; Duvic et al., 2012) probably act at a post-transcriptional level. About a half of the genes presented similar and significant induction profiles in the hemocytes and in the fat body. This is for instance the case of the usually anti-Gram negative bacteria attacin, cecropin and gloverin AMPs (Yi et al., 2014), which were all highly induced in the two tissues (Fig. 1A), suggesting they both respond to the bacterial partner *X. nematophila*. On the other hand, all the induced GNBP, lysozyme and LLP genes were found to be either significantly induced in the hemocytes or in the fat body, and in the AMP category, tissue-specificities were observed for diapausin, defensin-like and most moricin genes (Fig. 1A).

Only 8 antimicrobial response genes were found to be significantly downregulated (Fig. 1A). Interestingly, 4 were involved in the Imd pathway whereas the 4 remaining ones were dispersed between the AMP, GNBP and lysozyme categories (Fig. 1A). The Imd pathway downregulated factors included *sickie* and the *akirin* in the hemocytes and *SMARCC2* and *BAP60* in the fat body (Fig. 1A). In *D. melanogaster*, Sickie participates in the activation of Relish, the transcription factor of the Imd pathway (Foley and O'Farrell, 2004) and the akirin acts together with the Brahma chromatin-remodeling complex, containing BAP60 and SMARCC2, as cofactor of Relish to induce the expression of AMP genes (Bonnay et al., 2014). Only few data can be found in current literature on the transcriptional regulation of these factors (Bonnay et al., 2014; Cao et al. 2015; Chen et al., 2018). It is thus difficult to determine whether the downregulations we observed correspond to a normal negative feedback of the humoral immune response or to an immunosuppressive effect of the NBC. In a previous study on the *Spodoptera exigua* model, Hwang et al. (2013) have shown injection of live *X. nematophila* induces lower transcriptional inductions of several AMP genes than injection of dead bacteria (Hwang et al., 2013). It would be interesting to determine, either in the *S. exigua* or in the *S. frugiperda* model, whether reduction of AMP induction in response to live bacteria co-occurs with a downregulation of the Relish cofactors and activators we identified in the present analysis.

To summarize, the antimicrobial responses are potent and diversified in the two tissues, with a common induction of genes that probably respond to *X. nematophila*. Yet unexplained tissue-specific responses were observed and the results show a down-regulation of Imd pathway members that could be related to a previously described transcriptional immunosuppressive effect of the NBC. However, since at 15hpi, the full repertoire of *S. frugiperda* AMP is still expressed in response to naturally infesting NBC (Fig. 1A), this effect might not be potent enough to suppress the humoral response at this time point, suggesting that the NBC probably uses additional resistance and/or immunosuppressive strategies to survive the insect's humoral immune response.

3.1.2. Melanization

In the melanization category, 16 genes were found to be upregulated in at least one of the two tissues (Fig. 1B). These genes firstly encoded 6 serine proteases (Fig. 1B) that were considered as members of the prophenoloxidase (proPO) system. The proPO system is an extracellular proteolytic cascade ending in the maturation of the proPO zymogen into PO, which initiates the melanization process (Nakhleh et al., 2017). Among the upregulated serine proteases, PPAE2 is the only one that is known to take part in proPO processing whereas the other proteases were included in this category because of their characteristic CLIP domains and of their low homology with the serine proteases acting upstream of the Toll pathway in *D. melanogaster* (Veillard et al., 2016). The other upregulated genes in this category included 3 serpins, which are known to regulate the proPO system in several model insects (Nakhleh et al., 2017), 3 melanization enzymes, DDC, Yellow-like 1 and Punch-like (De Gregorio et al., 2001; Tang, 2009) as well as 4 genes, Reeler-1 and 3 Hdd23 homologs, that are involved in melanization and nodule formation in other models (Bao et al., 2011; Qiao et al., 2014) (Fig. 1B). Despite of tissue-specific induction patterns, serine proteases and serpins were found in the two tissues (Fig. 1B), suggesting that both participate in the stimulation of the proPO system, which is consistent with results obtained in other interaction models (Yuan et al., 2017; Zou et al., 2015; Zou et al., 2010). However, with the exception of the DDC, all the melanization enzymes as well as the nodulation-related genes were specifically induced in the hemocytes (Fig. 1B), which is consistent with the very localized nature of this immune response (Tang, 2009) that is mainly mediated by hemocyte subtypes.

Finally, only 2 genes, PPAE1 and Yellow-like 2, were found to be significantly down-regulated in this category (Fig. 1B). Both were specifically repressed in the hemocytes, which could be due to functional interferences with their upregulated homologs (PPAE2 and Yellow-like 1) and/or to an expression in specific hemocyte subtype(s) whose proportion in the total hemocyte population would influence the observed log2 fold changes. There is also the possibility of an immunosuppressive effect of the NBC on the expression of these genes.

In summary, our results suggest that both the hemocytes and the fat body participate in induction and regulation of melanization in response to the NBC and no clear sign of immunosuppression at the

transcriptional level is detected for this response. These results are in agreement with the previous identification of diverse inhibitors of PO activity in both *S. carpocapsae* (Balasubramanian et al., 2009; Balasubramanian et al., 2010) and *X. nematophila* (Crawford et al., 2012; Eom et al., 2014) that act at the post-transcriptional level.

3.1.3. Cellular responses

In the hemocytes, 19 upregulated genes were placed in the cellular responses category (Fig. 1C). The signaling ones encoded 3 homologs of the transcription factor Krüppel (Kr) (Fig. 1C). In *D. melanogaster*, Kr and Kr homologs are involved in several developmental processes such as embryo patterning (Schmucker et al., 1992), organogenesis (Fichelson et al., 2012; Harbecke and Janning, 1989; Hoch and Jackle, 1998), and cell differentiation (Ivy et al., 2015). More specifically in the hemocytes, Kr has been shown to take part in hemocytes' differentiation and/or activation (Stofanko et al., 2008), a crucial step for the induction of cellular immune responses. The recognition genes encoded 3 cellular receptors of the Scavenger (SR) and Integrin families plus the hemolin, a secreted immunoglobulin-containing protein (Fig. 1C). Both Scavenger receptors and integrins are known to act as membrane receptors in phagocytosis of bacteria and apoptotic cells (Nazario-Toole and Wu, 2017). In addition, integrins are involved in diverse processes, including cell motility and adhesion, and encapsulation (Levin et al., 2005; Melcarne et al., 2019). The hemolin is known to act as an opsonin by increasing phagocytosis and nodulation of bacteria in *Manduca sexta* (Eleftherianos et al., 2007). Among the effector genes, we first identified 5 upregulated genes corresponding to conserved intracellular phagocytosis-related proteins. They included Ced-6, the Rabenosyn-5 (Rbsn-5-like), a V-ATPase subunit (ATP6V0A2-like) and 2 small GTPase Activating Proteins (Rabex-5-like, CdGAPr-like) (Nazario-Toole and Wu, 2017) (Fig. 1C).We also found genes encoding membrane proteins, such as the immunoglobulin-containing hemicentin (HMCN-like) (Barat-Houari et al., 2006) and 4 tetraspanin-like (Tsp-like) proteins (Hemler, 2008) (Fig. 1C), that could participate in cell-cell adhesion and cellular immune responses. Interestingly, one of the upregulated tetraspanins (Tsp-like 3) presented 79.5% identity with the *Manduca sexta* (Lepidoptera : Noctuidae) tetraspanin D76, which takes part in hemocytes aggregation during capsule formation by trans-interacting with a specific integrin (Zhuang et al., 2007). Finally, 2 genes encoding proteins similar to the *D. melanogaster* clotting factors GP150 (Korayem et al., 2004) and a transglutaminase (Tg-like) (Lindgren et al., 2008) were also found upregulated (Fig. 1C). Only 2 genes (Ced-6-like, Rbsn-5-like) of the cellular responses category were found to be upregulated in the fat body (Fig. 1C) and both encoded intracellular proteins that are probably not related to immunity in this tissue.

All the 4 down-regulated putative cellular immunity-related genes were specifically modulated in the hemocytes (Fig. 1C). They encoded 2 Rho GTPase Activating Proteins (RhoGAP-like), a scavenger receptor similar to the *D. melanogaster* Croquemort receptor (SR-B3) and a homolog of the *D. melanogaster* integrin α-PS1. In *D. melanogaster*, Croquemort has been shown to take part in

phagocytosis of apoptotic cells and of the Gram positive bacterium *Staphylococcus aureus* but not of the Gram negative bacterium *Escherichia coli* (Melcarne et al., 2019; Stuart et al., 2005). Integrin α-PS1 is a ligand of the extracellular matrix protein laminin (Gotwals et al., 1994). It is involved in migration and differentiation of several cell types during development (Delon and Brown, 2009; Roote and Zusman, 1996; Urbano et al., 2011) but does not seem to be required for any immune process. Their down-regulations are thus probably due to their uselessness in the context of the response to the NBC.

Overall, the results suggest that all types of cellular responses are transcriptionally induced at 15 hpi, including phagocytosis and nodulation, as well as encapsulation that would be adapted to the bacterial partner or the nematode, respectively. In addition, the induction of coagulation responses is particularly interesting, since many clotting factors participate in *D. melanogaster* resistance to infestation by another type of NBC, the *Heterorhabditis bacteriophora-Photorhabdus luminescens* association (Arefin et al., 2014; Hyrsl et al., 2011; Kucerova et al., 2016; Wang et al., 2010). Moreover, despite *S. carpocapsae* does not pierce the insects' cuticles as *H. bacteriophora* (Dowds and Peters, 2002), it has been shown to express at least two secreted proteases with inhibitory activities towards the formation of clot fibers and coagulation-associated pathogen trapping (Toubarro et al., 2013a; Toubarro et al., 2013b). Once again, the induction of such immune responses is consistent with the previous identification of several virulence factors of the NBC targeting cellular immunity (Balasubramanian et al., 2009; Balasubramanian et al., 2010; Brivio et al., 2018; Eom et al., 2014; Kim et al., 2005; Park and Kim, 2000; Park and Stanley, 2006; Ribeiro et al., 1999; Ribeiro et al., 2003; Toubarro et al., 2013a; Vigneux et al., 2007).

3.1.4. Diverse immunity-related genes

A total of 29 modulated genes were involved in other diverse immune processes. They included 10 up- or down-regulated signaling genes, 7 upregulated recognition genes, 8 upregulated effector genes and 5 upregulated genes of unknown functions that are known to be modulated after immune challenge (Fig. 1D).

The signaling genes firstly encoded 2 insulin-like growth factor (IGF-II-like) and 2 insulin receptor substrate homologs (IRS1-like) (Fig. 1D). Insulin signaling is known to have a deleterious impact on the induction of systemic immune responses in the fat body of *D. melanogaster* (Lee and Lee, 2018) whereas insulin increases hemocyte proliferation in the hemolymph of mosquitoes (Castillo et al., 2011) as well as in the hematopoietic organs of the lepidopteran model *Bombyx mori* (Nakahara et al., 2006). In agreement with these assertions, we found that 2 of these genes were down-regulated in the fat body, but all 4 genes were upregulated in the hemocytes (Fig. 1D). Two other signaling genes were found to be specifically overexpressed in the hemocytes. The first one is a homolog of the *Litopenaeus vannamei* (Decapoda: Penaeidae) leucine-rich repeat flightless-I-interacting protein 2 (LRRFIP2-like) (Fig. 1D), which has been shown to upregulate AMP expression in *L. vannemei* as well as in *D. melanogaster* (Zhang et al., 2013). On the other hand, 3 signaling genes were found to be strictly down-regulated (Fig. 1D). Interestingly,

these genes included a member of the TGF-β pathway (BAMBI-like) in the hemocytes and a member of the JNK pathway in the fat body (Basket), two pleiotropic pathways that are currently suspected to take a part in the *D. melanogaster* immune response to nematodes after NBC infestation (Eleftherianos et al., 2016; Ozakman and Eleftherianos, 2019; Patrnogic et al., 2018; Yadav et al., 2018). The third down-regulated gene was found in the fat body and encoded MASK, an inducer of the Jak/Stat pathway (Fisher et al., 2018). In the fat body, the Jak-Stat pathway has mainly been shown to induce the expression of cytokines (Pastor-Pareja et al., 2008) and of a putative opsonin belonging to the TEP family (Lagueux et al., 2000). Remarkably, several TEP genes have been shown to participate in antibacterial immunity after NBC infestation in *D. melanogaster* (Arefin et al., 2014; Shokal and Eleftherianos, 2017; Shokal et al., 2017; Shokal et al., 2018). All of these down-regulations could thus impair the insect's immune response to the NBC. However, more detailed analyses of their functions and modulations would be required to hypothesize immunosuppressive effects of the NBCs.

All 7 upregulated recognition genes encoded lectins (Fig. 1D). Five of them encoded C-type lectins (CLECT), which are known to be involved in binding of diverse pathogens (Xia et al., 2018), including bacteria and nematodes (Yu and Kanost, 2004). This binding can then stimulate several immune responses, such as bacterial aggregation, melanization, phagocytosis, nodulation and encapsulation (Xia et al., 2018). The 2 others encoded galectins, which are involved in diverse aspects of mammalian immunity, including pathogens binding (Baum et al., 2014), and are considered as relevant candidate immune proteins in insects (Pace and Baum, 2002). Despite a larger set of upregulated lectins was identified in the fat body, members of these protein families were found upregulated in the two tissues.

In the hemocytes, the upregulated effector genes firstly encoded a homolog of the superoxide dismutase (SOD-like), a conserved detoxifying enzyme involved in responses to reactive oxygen species (Wang et al., 2018) (Fig. 1D). The 7 remaining genes encoded proteins with similarity to insect metalloproteinase inhibitors (IMPI-like) (Fig. 1D), whose functions have only been studied in the lepidopteran model *Galleria mellonella*. The only characterized IMPI encodes two proteins of which one is probably involved in the regulation of extracellular matrix remodeling and the second specifically targets metalloproteinases from pathogens (Wedde et al., 1998; Wedde et al., 2007). *S. carpocasape* and *X. nematophila* both express several secreted serine proteases as well as metalloproteinases during the infectious process (Caldas et al., 2002; Chang et al., 2019; Dillman et al., 2015; Hao et al., 2010; Jing et al., 2010; Lu et al., 2017; Massaoud et al., 2011). The induction of such immune responses could interfere with some of these proteinases to impair the NBC's virulence and/or survival. Interestingly, all but one of these IMPI homologs were found to be specifically upregulated in the hemocytes, a tissue-specificity that had not been highlighted in previous reports (Griesch et al., 2000; Vertyporokh and Wojda, 2017).

Finally, the remaining genes of unknown function encoded Spod-x-tox, a protein without antimicrobial activity which contains tandem repeats of defensin-like motifs (Destoumieux-Garzon et al., 2009), 3

REPAT genes, which are known to be induced in the midgut after exposure to toxins, viruses and intestinal microbiota perturbations in the close species *S. exigua* (Herrero et al., 2007; Navarro-Cerrillo et al., 2012; Navarro-Cerrillo et al., 2013), and Hdd1, which is induced in response to bacteria and peptidoglycan in the lepidopteran models *Hyphantria cunea* and *Bombyx mori* (Shin et al., 1998; Zhang et al., 2017) (Fig. 1D).

In summary, we found an important additional mobilization of several relevant candidate immune genes, including mainly insulin signaling factors and IMPIs in the hemocytes and lectins in the fat body. In addition, these results suggest that the candidate immune pathways TGF-β, JNK and Jak/Stat could be down-regulated. Such down-regulations are in disagreement with the results of Yadav and colleagues (Yadav et al., 2017) in *D. melanogaster* and thus would require further investigation.

3.2. Temporal analysis of the induced immune responses

In order to put the *S. frugiperda* immune responses in relation with the infectious process, we then described their temporal dynamics in each analyzed immunocompetent tissue. To this aim, we monitored with RT-qPCR experiments the induction levels of selected representative immune genes from 5 hpi, the mean time at which nematodes release *X. nematophila* in the hemocoel, to 20 hpi, which is about 9 hours before the first insect deaths (Supplementary Fig. 2).

In the hemocytes, the selected genes included 15 genes of the antimicrobial response, 2 genes involved in melanization, 5 cellular response genes, 2 lectins and one IMPI-like gene. At 5 hpi, only 2 genes, encoding a lebocin antibacterial (Yi et al., 2014) AMP (Lebocin 2) and the negative regulator Pirk of the Imd pathway (Kleino et al., 2008), were found to be significantly upregulated. However, most of the selected genes that are strongly induced at later time points also presented positive log2 fold changes at this time point (Fig. 2A). From 10 to 20 hpi, all selected genes but few exceptions (*cecropin D*, *Tg-like* and *Integrin β-like*) due to biological variability were significantly upregulated at each time point (Fig. 2A). Clustering analyses based on Pearson coefficients however revealed 3 distinct clusters of covariations. The first one contained 13 genes belonging to all the categories cited above and corresponded to very stable induction patterns (Fig. 2A). The second one, which contained 8 genes involved antimicrobial and cellular responses plus the selected C-type lectin (*CLECT (ccBV)*), corresponded to slightly increasing patterns (Fig. 2A). Finally, the third one, which contained the Relish and Pelle members of the Imd and Toll pathways (Ferrandon et al., 2007), an integrin and the DDC melanization enzyme (Huang et al., 2005) genes, corresponded to slightly decreasing patterns (Fig. 2A).

In the fat body, the selected genes included 15 genes of the antimicrobial response, 2 genes involved in melanization, one galectin gene (*Galectin 1*) and an IMPI-like gene (*IMPI-like 3*). At 5 hpi, all 7 selected AMPs, *PGRP-S1* and *Galectin 1* were found to be upregulated (Fig. 2B). All these genes were among the most strongly overexpressed at later time points. Such as in the hemocytes, most of the selected genes were then significantly upregulated from 10 to 20 hpi (Fig. 2B). In this tissue, the genes only subdivided

into two main covariation clusters: a cluster of genes with stable induction patterns and a cluster of genes with increasing induction patterns. The first cluster contained 10 genes of which 8 were involved in antimicrobial responses, one encoded a melanization-related serine protease (Snake-like 2) and one encoded the Galectin 1 (Fig. 2B). The second cluster contained 9 genes, of which 7 were involved in antimicrobial responses, one encoded the DDC melanization enzyme (Huang et al., 2005) and the last one encoded the IMPI-like 3 (Fig. 2B).

Altogether, the results obtained for the two tissues show that most of the transcriptional immune responses induced at 15 hpi take place between 0 and 10 hpi, which is comparable to timings observed in other interaction models (Boutros et al., 2002; Erler et al., 2011; Lemaitre et al., 1997). The results also indicate that these responses are globally stable across the time post-infestation despite some distinct gene induction patterns in each category of response. Interestingly, while we were hoping to discriminate between an early response, probably activated by the nematode presence, and a later response, probably reacting to bacterial growth, we did not find any clear link between the gene inductions' dynamics and the different immune processes and pathways that were represented in our selection.

3.3. Evaluation of each NBC partner's part in the induced immune responses

In order to identify each NBC partner's relative participation in the fat body's and hemocytes' immune responses, we used RT-qPCR to compare the induction levels of the selected immune genes after independent infections by the whole NBC, the axenic nematode or the bacterial symbiont. To this aim, we decided to use a more standardized protocol of direct injection of the pathogens into the hemocoel, thereby limiting putative side effects such as early hemocoel colonization by intestinal microorganisms. Importantly, we previously compared the kinetics of *X. nematophila* growth and of *S. frugiperda* survival after injection of the entire NBC and of 200 *X. nematophila* (Supplementary Fig. 3A,B). This comparison showed that both kinetics are very similar and thus that any difference of induction level between the 2 conditions would not reflect differences in bacterial load or physiological state. However, the putative impact of axenization on the nematode's physiology could not be assessed by the same way due to technical limitations and to its avirulence in absence of its bacterial symbiont (Supplementary Fig. 3B,C).

In the hemocytes, 14 genes presented higher induction levels in response to *X. nematophila* than in response to the axenic nematode (Fig. 3). In the antimicrobial category, they included the negative regulator *Pirk* of the Imd pathway (Kleino et al., 2008), all the selected attacin, cecropin, gloverin, lebocin and gallerimycin AMP genes, the 2 selected PGRP-S genes, and also probably the Imd pathway transcription factor *Relish* despite non-significant statistics (Ferrandon et al., 2007) (Fig. 3A). As indicated above, the Imd pathway, as well as the attacin, cecropin and gloverin AMP families, are known to take part in anti-Gram negative bacteria immune responses (Ferrandon, 2013; Yi et al., 2014). Their induction patterns thus indicate that the antimicrobial *X. nematophila*-induced responses are well adapted to the nature of the pathogen. Moreover, these results are in agreement with the study of Aymeric et al.

(2010) showing that the Imd pathway functions in the *D. melanogaster* immune response to *X. nematophila*. In the other categories, the *X. nematophila*-induced genes encoded the DDC melanization enzyme (Huang et al., 2005), the hemolin antibacterial opsonin (Eleftherianos et al., 2007), the IMPI-like 3, and also probably the selected integrin (Integrin β-like) (Fig. 3B-D). Once again, all of these genes are susceptible to play a part in an immune response to a pathogenic bacterium even though most of them could act on diverse types of invaders. Surprisingly, we found that *X. nematophila* strongly over-induces the transglutaminase (Tg-like) putative clotting factor gene (Lindgren et al., 2008) (Fig. 3C). This result could suggest that the bacterium is actually the main responsible for tissue damages at this time point and/or that *Tg-like* expression is induced in response to bacteria. Importantly, this result is in agreement with the study of Yadav and colleagues (Yadav et al., 2017), who showed that the *D. melanogaster* Fondue clotting factor was induced after infestation by the NBC but not after infestation by axenic nematodes. Remarkably, most of the genes that were mostly induced by *X. nematophila* presented higher induction values in response to the bacterium alone than in response to the whole NBC. However, this observation cannot be directly interpreted as an antagonistic effect of the nematode partner since it could be due to changes in the relative proportions of each hemocyte subtype, which would not necessarily reflect absolute variations in their numbers. In addition, the nematode partner specifically induced the overexpression of the selected C-type lectin (*CLECT (ccBV)*) and was probably the main inducer of the *Galectin 1*, the tetraspanin D76 homolog (*Tsp-like 3*) and the selected diapausin AMP (*Diapausin 5*) (Fig. 3A,C,D). As mentioned before, the *M. sexta* tetraspanin D76 is known to take part in encapsulation (Zhuang et al., 2007) and some lectins can bind nematodes and participate in melanization (Yu and Kanost, 2004) as well as in all types of cellular immune responses. Once again, their induction patterns are consistent with the nature of the pathogen, since both types of molecules could be involved in classical anti-nematode immune responses, such as cellular or melanotic encapsulation (Eleftherianos et al., 2017). Finally, 5 genes, encoding the Toll pathway members Pelle and Cactus (Ferrandon et al., 2007), the selected moricin AMP (Moricin 2), the melanization-related PPAE2 and the Krüppel-like transcription factor (Kr-like factor 1), were similarly induced by each of the three pathogens (Fig. 3A-C), suggesting that these responses are induced by the 2 partners without any additive effect.

In the fat body, statistical analysis of the results firstly revealed that the induction levels of *Pirk* as well as of the selected cecropin and gloverin AMP genes were significantly lower in response to the axenic nematode than in response to the NBC and to *X. nematophila* (Fig. 4A), suggesting the bacterial partner is the main responsible for their inductions. In addition, despite non-significant statistics, the results for the selected attacin AMPs, PGRP-S6 and GNBP3 genes showed similar induction patterns (Fig. 4A). As for the hemocytes, the induction patterns of *Pirk* and of the attacin, cecropin and gloverin AMP genes suggest that the fat body's antimicrobial response to *X. nematophila* is well adapted to the type of pathogen that is met. On the contrary, the induction levels of the melanization-related serine protease

(*Snake-like 2*) was significantly lower in response to *X. nematophila* than in response to the NBC and to the axenic nematode (Fig. 4B), suggesting that the nematode partner is the main responsible for its induction. Similar induction patterns were obtained for the Toll pathway members *Toll* and *Cactus* (Ferrandon et al., 2007) as well as for *Galectin 1* (Fig. 4A,C). As mentioned for the hemocytes, the induction of lectins and melanization-related genes in response to the nematode is consistent with the nature of the pathogen since both could participate in classical anti-nematode immune responses (Eleftherianos et al., 2017). The induction of Toll pathway members is more difficult to relate with known anti-nematode immune responses and Yadav et al. (2018) found that the inactivation of this pathway does not impact the *D. melanogaster* survival to infestation by the whole NBC or by axenic *S. carpocapsae*. However, the involvement of this immune pathway in anti-nematode immune responses may depend on the downstream effectors and thus be variable between insect species. Finally, the other genes did not show any clear difference of induction level after injection of the 3 pathogens, except for the gallerimycin AMP, PGRP-S1 and the DDC melanization enzyme genes, which presented a lower induction when each NBC partner was injected alone (Fig. 4A,B). These results suggest synergistic effects of the nematode and of the bacterium on the induction of these genes.

In summary, we found in the 2 tissues that most of the selected genes presented partner-specific induction patterns, suggesting that the immune response to the NBC corresponds to combinations of responses induced by each partner. The detailed analysis of these genes indicates that *X. nematophila* is the main inducer of most of the selected genes, and especially of the well-known antibacterial ones. On the other hand, *S. carpocapsae* is the main inducer of some melanization and encapsulation-related genes and of the selected lectins, which could all take part in classical anti-nematode immune responses. The results thus globally suggest that the hemocytes and the fat body both respond appropriately to each NBC partner despite some yet unexplained results, such as an induction of Toll pathway members in the fat body by the nematode partner.

3.4. Expression patterns of two new clusters of candidate immune genes

During our first analysis of the RNAseq data, we identified 2 new clusters of candidate immune genes (Huot et al., 2019). The first one, named the Unknown (Unk) cluster, was localized close to *Tamozhennic*, a gene encoding a nuclear porin involved in the nucleation of Dorsal, the transcription factor of the Toll pathway (Minakhina et al., 2003). It contained 5 genes predicted to encode secreted peptides and short proteins that were all highly overexpressed in the midgut, fat body and hemocytes at 15 hpi and of which 4 were the unique mobilized genes at 8 hpi in the fat body. The second cluster, named the Genes with Bacterial Homology (GBH) cluster, contained 3 genes located inside a defensin-like AMP genes cluster in the *S. frugiperda* genome. The 3 genes were predicted to encode secreted proteins similar to each other and one of them was also found highly induced at 15 hpi in the 3 tissues. The particularity of these genes is that homologs are found only in lepidopteran species as well as, intriguingly, in Gram positive bacteria.

Here, we reexamined the expression patterns of the *Unk* and *GBH* genes and found that the 5 *Unk* genes were mainly expressed in the fat body whereas 2 of the 3 *GBH* genes were mainly expressed and induced in the hemocytes (Supplementary Table 3).

In order to learn more about their putative functions, we decided to analyze, as we did for the known immune genes, their induction patterns across the time post-infestation and in response to each NBC partner in the corresponding tissues. In both cases, we found that the induction dynamics of the genes were very similar to those of immune genes, with an upregulation that becomes significant at 5 or 10 hpi and with globally stable induction patterns from 10 to 20 hpi (Fig. 5A,B).

In the case of the GBH cluster, the results that we got for the 2 NBC-responsive genes (*GBH1* and *GBH3*) in the hemocytes indicate that they are significantly less induced after axenic nematode injection than after NBC and *X. nematophila* injections, suggesting that the bacterium is the main responsible for their up-regulation (Fig. 5C). We could hypothesize an acquisition by horizontal gene transfer from bacteria of the *GBH* genes. In this case, their putative involvement in the antibacterial immune response would be particularly interesting, since bacterial genes hijacking for immune purpose has only been reported once in metazoans, in the tick *Ixodes scapularis* (Chou et al., 2015). Such a hypothesis however requires functional confirmation.

In the case of the Unk cluster, we found that the 4 most induced genes in the fat body (*Unk2* to *5*) are all strongly and similarly induced by the NBC and by the axenic nematode whereas they are not induced by *X. nematophila* (Fig. 5D). The results are very similar for the least expressed *Unk* gene (*Unk1*), for which we only found a significant induction for the injection of axenic nematodes (Fig. 5D). This partner-specific induction pattern suggests that the *Unk* genes are involved in specific aspects of the insect responses to the infestation. In addition, the putative involvement of the *Unk* genes in the response to the nematode partner seems to be in agreement with their early mobilization during the infectious process and with their overexpression in the midgut (Huot et al., 2019), which is the entry site of the nematode. In our previous study, we had hypothesized the *Unk* genes may encode new types of immune effectors (Huot et al., 2019). However, given their low levels of conservation in species as close as *S. litura* or *S. littoralis* (Supplementary Fig. 4) another hypothesis would be that they correspond to regulatory long non-coding RNAs (Johnsson et al., 2014; Qu and Adelson, 2012). In both cases, the further functional characterization of these genes could be very promising given our current lack of knowledge of the immune pathways and molecular effectors of insect anti-nematode immunity.

4. Conclusion

Here, we provide a very deep and contextualized analysis of the *S. frugiperda*'s hemocytes' and fat body's transcriptional immune responses to infestation by the *S. carpocapsae-X. nematophila* NBC. Our topologic analysis of these responses at 15 hpi firstly confirmed the induction of very potent and

diversified immune responses towards the pathogen, such as suggested by our previous analysis of the transcriptomic data (Huot et al., 2019) as well as by the study of Yadav et al. (2017) in the *D. melanogaster* model. The present work now shows that these responses are very stable across the post-infestation time and that they correspond to combinations of *X. nematophila*- and *S. carpocapsae*-induced responses that seem to be well adapted to the nature of each partner (Figure 6).

Together with results obtained in other insect models, the pieces of information collected during these analyses are of great interest for the study of the dialogue that takes place between each NBC partner and *S. frugiperda*'s immune systems. First, our results strongly suggest that the NBC immunosuppressive strategies globally have a low impact on the induction of immune responses at the transcriptional level in *S. frugiperda*. They also indicate that the nematode and/or its effects on the host are detected by the insect's immune system that in return seems to induce appropriate immune responses towards the pathogen. Such observations could help to determine the limits and/or universality of previously described immunosuppressive and immunoevasive strategies of the NBC that have been described in other models. For example, they suggest that the suppressive effect of *X. nematophila* on the expression of AMP genes (Hwang et al., 2013; Ji and Kim, 2004; Park et al., 2007) as well as the camouflage strategy of *S. carpocapsae* (Binda-Rossetti et al., 2016; Mastore et al., 2015) are probably far from sufficient to explain their success towards the *S. frugiperda*'s immune system, which could also be true for other insect species. On the other hand, we found several unexplained down-regulations of signaling genes, such as of members of the Imd, JNK, TGF-β and Jak-Stat pathways, that had never been reported before and which could open new working trails for the study of the molecular basis of the NBC's immunosuppressive strategies. Finally, this study allowed the identification of very large panels of candidate immune genes involved in all the main components of insect immunity as well as of some yet uncharacterized genes that could encode new immune factors involved in the response to NBCs, such as the *GBH* and the *Unk* genes, which are respectively specific to lepidopterans and to some noctuid species (Huot et al., 2019).

Continuing this work with more functional and mechanistic approaches is now required to get an accurate picture of the molecular dialogue between the NBC and the immune system. In the longer term, using such detailed and contextualized approaches on diverse insect species could help to identify the precise causes of immune systems' failure or success towards this NBC and thus the conditions that are required for an adequate use of this pathogen against insect pests.

Acknowledgments

We thank the quarantine insect platform (PIQ), member of the Vectopole Sud network, for providing the infrastructure needed for pest insect experimentations. We are also grateful to Clotilde Gibard, Raphaël Bousquet and Gaëtan Clabots for maintaining the insect collections of the DGIMI laboratory in

Montpellier. This work was supported by grants from the French Institut National de la Recherche Agronomique.

Authors' contribution

L.H., N.N. and B.D. conceived this study. N.N. and B.D. directed this study. L.H. and P.-A.G. performed the infestation experiments. L.H., P.-A.G. performed dissections. L.H. and A.B. extracted and purified the RNA. J.-C.O. designed the *X. nematophila* specific primers. S.P. produced the axenic nematodes and checked their axenization. L.H. and A.B. performed the qPCRs. L.H., N.N. and B.D. analysed the data. L.H. wrote the manuscript. L.H., N.N. and B.D. revised the manuscript. All authors have read and approved the manuscript.

Additional Information

Competing Interests: The authors declare no competing interests.

References

Arefin, B., Kucerova, L., Dobes, P., Markus, R., Strnad, H., Wang, Z., Hyrsl, P., Zurovec, M., Theopold, U., 2014. Genome-wide transcriptional analysis of *Drosophila* larvae infected by entomopathogenic nematodes shows involvement of complement, recognition and extracellular matrix proteins. J Innate Immun 6, 192-204, 10.1159/000353734.

Aymeric, J.L., Givaudan, A., Duvic, B., 2010. Imd pathway is involved in the interaction of *Drosophila melanogaster* with the entomopathogenic bacteria, *Xenorhabdus nematophila* and *Photorhabdus luminescens*. Mol Immunol 47, 2342-2348, 10.1016/j.molimm.2010.05.012.

Balasubramanian, N., Hao, Y.J., Toubarro, D., Nascimento, G., Simoes, N., 2009. Purification, biochemical and molecular analysis of a chymotrypsin protease with prophenoloxidase suppression activity from the entomopathogenic nematode *Steinernema carpocapsae*. Int J Parasitol 39, 975-984, 10.1016/j.ijpara.2009.01.012.

Balasubramanian, N., Toubarro, D., Simoes, N., 2010. Biochemical study and *in vitro* insect immune suppression by a trypsin-like secreted protease from the nematode *Steinernema carpocapsae*. Parasite Immunol 32, 165-175, 10.1111/j.1365-3024.2009.01172.x.

Bao, Y.Y., Xue, J., Wu, W.J., Wang, Y., Lv, Z.Y., Zhang, C.X., 2011. An immune-induced Reeler protein is involved in the *Bombyx mori* melanization cascade. Insect Biochem Mol Biol 41, 696-706, 10.1016/j.ibmb.2011.05.001.

Barat-Houari, M., Hilliou, F., Jousset, F.X., Sofer, L., Deleury, E., Rocher, J., Ravallec, M., Galibert, L., Delobel, P., Feyereisen, R., Fournier, P., Volkoff, A.N., 2006. Gene expression profiling of *Spodoptera frugiperda* hemocytes and fat body using cDNA microarray reveals polydnavirus-associated variations in lepidopteran host genes transcript levels. BMC Genomics 7, 10.1186/1471-2164-7-160.

Baum, L.G., Garner, O.B., Schaefer, K., Lee, B., 2014. Microbe-host interactions are positively and negatively regulated by galectin glycan interactions. Front Immunol 5, 10.3389/Fimmu.2014.00284.

Binda-Rossetti, S., Mastore, M., Protasoni, M., Brivio, M.F., 2016. Effects of an entomopathogen nematode on the immune response of the insect pest red palm weevil: Focus on the host antimicrobial response. J Invertebr Pathol 133, 110-119, 10.1016/j.jip.2015.11.001.

Boemare, N., Thaler, J.O., Lanois, A., 1997. Simple bacteriological tests for phenotypic characterization of *Xenorhabdus* and *Photorhabdus* phase variants. Symbiosis 22, 167-175.

Bonnay, F., Nguyen, X.H., Cohen-Berros, E., Troxler, L., Batsche, E., Camonis, J., Takeuchi, O., Reichhart, J.M., Matt, N., 2014. Akirin specifies NF-κB selectivity of *Drosophila* innate immune response via chromatin remodeling. EMBO J 33, 2349-2362, 10.15252/embj.201488456.

Boutros, M., Agaisse, H., Perrimon, N., 2002. Sequential activation of signaling pathways during innate immune responses in *Drosophila*. Dev Cell 3, 711-722, 10.1016/S1534-5807(02)00325-8.

Bray, N.L., Pimentel, H., Melsted, P., Pachter, L., 2016. Near-optimal probabilistic RNA-seq quantification. Nat Biotechnol 34, 525-527, 10.1038/nbt.3519.

Brey, P.T., Lee, W.J., Yamakawa, M., Koizumi, Y., Perrot, S., Francois, M., Ashida, M., 1993. Role of the integument in insect immunity - Epicuticular abrasion and induction of cecropin synthesis in cuticular epithelial-cells. Proc Natl Acad Sci USA 90, 6275-6279, 10.1073/pnas.90.13.6275.

Brivio, M.F., Toscano, A., De Pasquale, S.M., Barbaro, A.D., Giovannardi, S., Finzi, G., Mastore, M., 2018. Surface protein components from entomopathogenic nematodes and their symbiotic bacteria: effects on immune responses of the greater wax moth, *Galleria mellonella* (Lepidoptera: Pyralidae). Pest Manag Sci 74, 2089-2099, 10.1002/ps.4905.

Caldas, C., Cherqui, A., Pereira, A., Simoes, N., 2002. Purification and characterization of an extracellular protease from *Xenorhabdus nematophila* involved in insect immunosuppression. Appl Environ Microbiol 68, 1297-1304, 10.1128/Aem.68.3.1297-1304.2002.

Cambon, M., Lafont, P., Frayssinet, M., Lanois, A., Ogier, J.C., Pagès, S., Parthuisot, N., Ferdy, J.B., Gaudriault, S., 2020. Bacterial community profile after the lethal infection of *Steinernema-Xenorhabdus* pairs into soil-reared *Tenebrio molitor* larvae. FEMS Microbiol Ecol, 10.1093/femsec/fiaa009.

Cao, X., He, Y., Hu, Y., Wang, Y., Chen, Y.R., Bryant, B., Clem, R.J., Schwartz, L.M., Blissard, G., Jiang, H., 2015. The immune signaling pathways of *Manduca sexta*. Insect Biochem Mol Biol 62, 64–74, 10.1016/j.ibmb.2015.03.006.

Castillo, J., Brown, M.R., Strand, M.R., 2011. Blood feeding and insulin-like peptide 3 stimulate proliferation of hemocytes in the mosquito *Aedes aegypti*. PLoS Pathog 7, e1002274, 10.1371/journal.ppat.1002274.

Chang, D.Z., Serra, L., Lu, D., Mortazavi, A., Dillman, A.R., 2019. A core set of venom proteins is released by entomopathogenic nematodes in the genus *Steinernema*. PLoS Pathog 15, e1007626, 10.1371/journal.ppat.1007626.

Chen, T.T., Tan, L.R., Hu, N., Dong, Z.Q., Hu, Z.G., Jiang, Y.M., Chen, P., Pan, M.H., Lu, C., 2018. C-lysozyme contributes to antiviral immunity in *Bombyx mori* against nucleopolyhedrovirus infection. J Insect Physiol 108, 54-60, 10.1016/j.jinsphys.2018.05.005.

Chou, S., Daugherty, M.D., Peterson, S.B., Biboy, J., Yang, Y.Y., Jutras, B.L., Fritz-Laylin, L.K., Ferrin, M.A., Harding, B.N., Jacobs-Wagner, C., Yang, X.F., Vollmer, W., Malik, H.S., Mougous, J.D., 2015. Transferred interbacterial antagonism genes augment eukaryotic innate immune function. Nature 518, 98-101, 10.1038/nature13965.

Conesa, A., Gotz, S., Garcia-Gomez, J.M., Terol, J., Talon, M., Robles, M., 2005. Blast2GO: a universal tool for annotation, visualization and analysis in functional genomics research. Bioinformatics 21, 3674-3676, 10.1093/bioinformatics/bti610.

Crawford, J.M., Portmann, C., Zhang, X., Roeffaers, M.B.J., Clardy, J., 2012. Small molecule perimeter defense in entomopathogenic bacteria. Proc Natl Acad Sci USA 109, 10821-10826, 10.1073/pnas.1201160109.

De Gregorio, E., Spellman, P.T., Rubin, G.M., Lemaitre, B., 2001. Genome-wide analysis of the *Drosophila* immune response by using oligonucleotide microarrays. Proc Natl Acad Sci USA 98, 12590-12595, 10.1073/pnas.221458698.

Delon, I., Brown, N.H., 2009. The integrin adhesion complex changes its composition and function during morphogenesis of an epithelium. J Cell Sci 122, 4363-4374, 10.1242/jcs.055996.

Destoumieux-Garzon, D., Brehelin, M., Bulet, P., Boublik, Y., Girard, P.A., Baghdiguian, S., Zumbihl, R., Escoubas, J.M., 2009. *Spodoptera frugiperda* X-tox protein, an immune related defensin rosary, has lost the function of ancestral defensins. PLoS One 4, e6795, 10.1371/journal.pone.0006795.

Dillman, A.R., Macchietto, M., Porter, C.F., Rogers, A., Williams, B., Antoshechkin, I., Lee, M.M., Goodwin, Z., Lu, X.J., Lewis, E.E., Goodrich-Blair, H., Stock, S.P., Adams, B.J., Sternberg, P.W., Mortazavi, A., 2015. Comparative genomics of *Steinernema* reveals deeply conserved gene regulatory networks. Genome Biol 16, 10.1186/s13059-015-0746-6.

Dowds, B.C.A., Peters, A., 2002. Virulence Mechanisms, in Entomopathogenic Nematology, Gaugler, R. (Ed.). CABI Publishing, pp. 79-93.

Duvic, B., Jouan, V., Essa, N., Girard, P.A., Pages, S., Khattar, Z.A., Volkoff, N.A., Givaudan, A., Destoumieux-Garzon, D., Escoubas, J.M., 2012. Cecropins as a marker of *Spodoptera frugiperda* immunosuppression during entomopathogenic bacterial challenge. J Insect Physiol 58, 881-888, 10.1016/j.jinsphys.2012.04.001.

Eleftherianos, I., Castillo, J.C., Patrnogic, J., 2016. TGF-β signaling regulates resistance to parasitic nematode infection in *Drosophila melanogaster*. Immunobiology 221, 1362-1368, 10.1016/j.imbio.2016.07.011.

Eleftherianos, I., Gokcen, F., Felfoldi, G., Millichap, P.J., Trenczek, T.E., ffrench-Constant, R.H., Reynolds, S.E., 2007. The immunoglobulin family protein Hemolin mediates cellular immune responses to bacteria in the insect *Manduca sexta*. Cell Microbiol 9, 1137-1147, 10.1111/j.1462-5822.2006.00855.x.

Eleftherianos, I., Shokal, U., Yadav, S., Kenney, E., Maldonado, T., 2017. Insect immunity to entomopathogenic nematodes and their mutualistic bacteria. Curr Top Microbiol Immunol 402, 123-156, 10.1007/82_2016_52.

Eom, S., Park, Y., Kim, Y., 2014. Sequential immunosuppressive activities of bacterial secondary metabolites from the entomopahogenic bacterium *Xenorhabdus nematophila*. J Microbiol 52, 161-168, 10.1007/s12275-014-3251-9.

Erler, S., Popp, M., Lattorff, H.M.G., 2011. Dynamics of immune system gene expression upon bacterial challenge and wounding in a social insect (*Bombus terrestris*). PLoS One 6, e18126, 10.1371/journal.pone.0018126.

Ferrandon, D., 2013. The complementary facets of epithelial host defenses in the genetic model organism *Drosophila melanogaster*: from resistance to resilience. Curr Opin Immunol 25, 59-70, 10.1016/j.coi.2012.11.008.

Ferrandon, D., Imler, J.L., Hetru, C., Hoffmann, J.A., 2007. The *Drosophila* systemic immune response: sensing and signalling during bacterial and fungal infections. Nat Rev Immunol 7, 862-874, 10.1038/nri2194.

Fichelson, P., Brigui, A., Pichaud, F., 2012. Orthodenticle and Krüppel homolog 1 regulate *Drosophila* photoreceptor maturation. Proc Natl Acad Sci USA 109, 7893-7898, 10.1073/pnas.1120276109.

Fisher, K.H., Fragiadaki, M., Pugazhendhi, D., Bausek, N., Arredondo, M.A., Thomas, S.J., Brown, S., Zeidler, M.P., 2018. A genome-wide RNAi screen identifies MASK as a positive regulator of cytokine receptor stability. J Cell Sci 131, 10.1242/jcs.209551.

Foley, E., O'Farrell, P.H., 2004. Functional dissection of an innate immune response by a genome-wide RNAi screen. PLoS Biol 2, 1091-1106, 10.1371/journal.pbio.0020203.

Forst, S., Clarke, D., 2002. Bacteria–nematode symbiosis, in Entomopathogenic Nematology, Gaugler, R. (Ed.). CABI Publishing, pp. 57-78.

Galko, M.J., Krasnow, M.A., 2004. Cellular and genetic analysis of wound healing in *Drosophila* larvae. PLoS Biol 2, 1114-1126, 10.1371/journal.pbio.0020239.

Gandhe, A.S., Janardhan, G., Nagaraju, J., 2007. Immune upregulation of novel antibacterial proteins from silkmoths (Lepidoptera) that resemble lysozymes but lack muramidase activity. Insect Biochem Mol Biol 37, 655-666, 10.1016/j.ibmb.2007.03.013.

Ganger, M.T., Dietz, G.D., Ewing, S.J., 2017. A common base method for analysis of qPCR data and the application of simple blocking in qPCR experiments. BMC Bioinformatics 18, 534, 10.1186/s12859-017-1949-5.

Gotwals, P.J., Fessler, L.I., Wehrli, M., Hynes, R.O., 1994. *Drosophila* PS1 integrin is a laminin receptor and differs in ligand specificity from PS2. Proc Natl Acad Sci USA 91, 11447-11451, 10.1073/pnas.91.24.11447.

Gotz, P., Boman, A., Boman, H.G., 1981. Interactions between insect immunity and an insect-pathogenic nematode with symbiotic bacteria. Proc R Soc B 212, 333-350, 10.1098/rspb.1981.0043.

Gouin, A., Bretaudeau, A., Nam, K., Gimenez, S., Aury, J.M., Duvic, B., Hilliou, F., Durand, N., Montagne, N., Darboux, I., Kuwar, S., Chertemps, T., Siaussat, D., Bretschneider, A., Mone, Y., Ahn, S.J., Hanniger, S., Grenet, A.S.G., Neunemann, D., Maumus, F., Luyten, I., Labadie, K., Xu, W., Koutroumpa, F., Escoubas, J.M., Llopis, A., Maibeche-Coisne, M., Salasc, F., Tomar, A., Anderson, A.R., Khan, S.A., Dumas, P., Orsucci, M., Guy, J., Belser, C., Alberti, A., Noel, B., Couloux, A., Mercier, J., Nidelet, S., Dubois, E., Liu, N.Y., Boulogne, I., Mirabeau, O., Le Goff, G., Gordon, K., Oakeshott, J., Consoli, F.L., Volkoff, A.N., Fescemyer, H.W., Marden, J.H., Luthe, D.S., Herrero, S., Heckel, D.G., Wincker, P., Kergoat, G.J., Amselem, J., Quesneville, H., Groot, A.T., Jacquin-Joly, E., Negre, N., Lemaitre, C., Legeai, F., d'Alencon, E., Fournier, P., 2017. Two genomes of highly polyphagous lepidopteran pests (*Spodoptera frugiperda*, Noctuidae) with different host-plant ranges. Sci Rep 7, 11816, 10.1038/S41598-017-10461-4.

Griesch, J., Wedde, M., Vilcinskas, A., 2000. Recognition and regulation of metalloproteinase activity in the haemolymph of *Galleria mellonella*: a new pathway mediating induction of humoral immune responses. Insect Biochem Mol Biol 30, 461-472, 10.1016/S0965-1748(00)00010-2.

Ha, E.M., Lee, K.A., Park, S.H., Kim, S.H., Nam, H.J., Lee, H.Y., Kang, D., Lee, W.J., 2009. Regulation of DUOX by the Gαq-phospholipase Cβ-Ca^{2+} pathway in *Drosophila* gut immunity. Dev Cell 16, 386-397, 10.1016/j.devcel.2008.12.015.

Hao, Y.J., Montiel, R., Abubucker, S., Mitreva, M., Simoes, N., 2010. Transcripts analysis of the entomopathogenic nematode *Steinernema carpocapsae* induced *in vitro* with insect haemolymph. Mol Biochem Parasit 169, 79-86, 10.1016/j.molbiopara.2009.10.002.

Harbecke, R., Janning, W., 1989. The segmentation gene Krüppel of *Drosophila melanogaster* has homeotic properties. Gene Dev 3, 114-122, 10.1101/Gad.3.1.114.

Hemler, M.E., 2008. Targeting of tetraspanin proteins - potential benefits and strategies. Nat Rev Drug Discov 7, 747-758, 10.1038/nrd2659.

Herrero, S., Ansems, M., Van Oers, M.M., Vlak, J.M., Bakker, P.L., de Maagd, R.A., 2007. REPAT, a new family of proteins induced by bacterial toxins and baculovirus infection in *Spodoptera exigua*. Insect Biochem Mol Biol 37, 1109-1118, 10.1016/j.ibmb.2007.06.007.

Hoch, M., Jackle, H., 1998. Krüppel acts as a developmental switch gene that mediates Notch signalling-dependent tip cell differentiation in the excretory organs of *Drosophila*. EMBO J 17, 5766-5775, 10.1093/emboj/17.19.5766.

Huang, C.Y., Chou, S.Y., Bartholomay, L.C., Christensen, B.M., Chen, C.C., 2005. The use of gene silencing to study the role of dopa decarboxylase in mosquito melanization reactions. Insect Mol Biol 14, 237-244, 10.1111/j.1365-2583.2004.00552.x.

Huot, L., George, S., Girard, P.A., Severac, D., Negre, N., Duvic, B., 2019. *Spodoptera frugiperda* transcriptional response to infestation by *Steinernema carpocapsae*. Sci Rep 9, 12879, 10.1038/s41598-019-49410-8.

Hwang, J., Park, Y., Kim, Y., Hwang, J., Lee, D., 2013. An entomopathogenic bacterium, *Xenorhabdus nematophila*, suppresses expression of antimicrobial peptides controlled by Toll and Imd pathways by blocking eicosanoid biosynthesis. Arch Insect Biochem Physiol 83, 151-169, 10.1002/arch.21103.

Hyrsl, P., Dobes, P., Wang, Z., Hauling, T., Wilhelmsson, C., Theopold, U., 2011. Clotting factors and eicosanoids protect against nematode infections. J Innate Immun 3, 65-70, 10.1159/000320634.

Issa, N., Guillaumot, N., Lauret, E., Matt, N., Schaeffer-Reiss, C., Van Dorsselaer, A., Reichhart, J.M., Veillard, F., 2018. The circulating protease Persephone is an immune sensor for microbial proteolytic activities upstream of the *Drosophila* Toll pathway. Mol Cell 69, 539-550, 10.1016/j.molcel.2018.01.029.

Ivy, J.R., Drechsler, M., Catterson, J.H., Bodmer, R., Ocorr, K., Paululat, A., Hartley, P.S., 2015. Klf15 is critical for the development and differentiation of *Drosophila* nephrocytes. PLoS One 10, e0134620, 10.1371/journal.pone.0134620.

Ji, D.J., Kim, Y., 2004. An entomopathogenic bacterium, *Xenorhabdus nematophila*, inhibits the expression of an antibacterial peptide, cecropin, of the beet armyworm, *Spodoptera exigua*. J Insect Physiol 50, 489-496, 10.1016/j.jinsphys.2004.03.005.

Jing, Y.J., Toubarro, D., Hao, Y.J., Simoes, N., 2010. Cloning, characterisation and heterologous expression of an astacin metalloprotease, Sc-AST, from the entomoparasitic nematode *Steinernema carpocapsae*. Mol Biochem Parasit 174, 101-108, 10.1016/j.molbiopara.2010.07.004.

Jiravanichpaisal, P., Lee, B.L., Soderhall, K., 2006. Cell-mediated immunity in arthropods: Hematopoiesis, coagulation, melanization and opsonization. Immunobiology 211, 213-236, 10.1016/j.imbio.2005.10.015.

Johnsson, P., Lipovich, L., Grander, D., Morris, K.V., 2014. Evolutionary conservation of long non-coding RNAs: Sequence, structure, function. Biochim Biophys Acta Gen Subj 1840, 1063-1071, 10.1016/j.bbagen.2013.10.035.

Kim, Y., Ji, D., Cho, S., Park, Y., 2005. Two groups of entomopathogenic bacteria, *Photorhabdus* and *Xenorhabdus*, share an inhibitory action against phospholipase A_2 to induce host immunodepression. J Invertebr Pathol 89, 258-264, 10.1016/j.jip.2005.05.001.

Kleino, A., Myllymaki, H., Kallio, J., Vanha-aho, L.M., Oksanen, K., Ulvila, J., Hultmark, D., Valanne, S., Ramet, M., 2008. Pirk is a negative regulator of the *Drosophila* Imd pathway. J Immunol 180, 5413-5422, 10.4049/jimmunol.180.8.5413.

Korayem, A.M., Fabbri, M., Takahashi, K., Scherfer, C., Lindgren, M., Schmidt, O., Ueda, R., Dushay, M.S., Theopold, U., 2004. A *Drosophila* salivary gland mucin is also expressed in immune tissues: evidence for a function in coagulation and the entrapment of bacteria. Insect Biochem Mol Biol 34, 1297-1304, 10.1016/j.ibmb.2004.09.001.

Kristensen, N., Chauvin, G., 2012. Lepidoptera, moths and butterflies: Morphology, physiology, and development. Integument, in Handbook of Zoology, De Gruyter, W. (Ed.). Berlin: De Gruyter, pp. 1-8.

Kucerova, L., Broz, V., Arefin, B., Maaroufi, H.O., Hurychova, J., Strnad, H., Zurovec, M., Theopold, U., 2016. The *Drosophila* chitinase-like protein IDGF3 is involved in protection against nematodes and in wound healing. J Innate Immun 8, 199-210, 10.1159/000442351.

Labaude, S., Griffin, C.T., 2018. Transmission success of entomopathogenic nematodes used in pest control. Insects 9, E72, 10.3390/insects9020072.

Lacey, L.A., Grzywacz, D., Shapiro-Ilan, D.I., Frutos, R., Brownbridge, M., Goettel, M.S., 2015. Insect pathogens as biological control agents: Back to the future. J Invertebr Pathol 132, 1-41, 10.1016/j.jip.2015.07.009.

Lagueux, M., Perrodou, E., Levashina, E.A., Capovilla, M., Hoffmann, J.A., 2000. Constitutive expression of a complement-like protein in Toll and JAK gain-of-function mutants of *Drosophila*. Proc Natl Acad Sci USA 97, 11427-11432, 10.1073/pnas.97.21.11427.

Lee, K.A., Lee, W.J., 2018. Immune-metabolic interactions during systemic and enteric infection in *Drosophila*. Curr Opin Insect Sci 29, 21-26, 10.1016/j.cois.2018.05.014.

Lehane, M.J., 1997. Peritrophic matrix structure and function. Annu Rev Entomol 42, 525-550, 10.1146/annurev.ento.42.1.525.

Lemaitre, B., Reichhart, J.M., Hoffmann, J.A., 1997. *Drosophila* host defense: Differential induction of antimicrobial peptide genes after infection by various classes of microorganisms. Proc Natl Acad Sci USA 94, 14614-14619, 10.1073/pnas.94.26.14614.

Levin, D.M., Breuer, L.N., Zhuang, S.F., Anderson, S.A., Nardi, J.B., Kanost, M.R., 2005. A hemocyte-specific integrin required for hemocytic encapsulation in the tobacco hornworm, *Manduca sexta*. Insect Biochem Mol Biol 35, 369-380, 10.1016/j.ibmb.2005.01.003.

Li, X.Y., Cowles, R.S., Cowles, E.A., Gaugler, R., Cox-Foster, D.L., 2007. Relationship between the successful infection by entomopathogenic nematodes and the host immune response. Int J Parasitol 37, 365-374, 10.1016/j.ijpara.2006.08.009.

Lindgren, M., Riazi, R., Lesch, C., Willielinsson, C., Theopold, U., Dushay, M.S., 2008. Fondue and transglutaminase in the *Drosophila* larval clot. J Insect Physiol 54, 586-592, 10.1016/j.jinsphys.2007.12.008.

Lu, D., Macchietto, M., Chang, D., Barros, M.M., Baldwin, J., Mortazavi, A., Dillman, A.R., 2017. Activated entomopathogenic nematode infective juveniles release lethal venom proteins. PLoS Pathog 13, e1006302, 10.1371/journal.ppat.1006302.

Massaoud, M.K., Marokhazi, J., Venekei, I., 2011. Enzymatic characterization of a serralysin-like metalloprotease from the entomopathogen bacterium, *Xenorhabdus*. Biochim Biophys Acta-Proteins Proteom 1814, 1333-1339, 10.1016/j.bbapap.2011.05.008.

Mastore, M., Arizza, V., Manachini, B., Brivio, M.F., 2015. Modulation of immune responses of *Rhynchophorus ferrugineus* (Insecta: Coleoptera) induced by the entomopathogenic nematode *Steinernema carpocapsae* (Nematoda: Rhabditida). Insect Sci 22, 748-760, 10.1111/1744-7917.12141.

Melcarne, C., Lemaitre, B., Kurant, E., 2019. Phagocytosis in *Drosophila*: From molecules and cellular machinery to physiology. Insect Biochem Mol Biol 109, 1-12, 10.1016/j.ibmb.2019.04.002.

Minakhina, S., Yang, J., Steward, R., 2003. Tamo selectively modulates nuclear import in *Drosophila*. Genes Cells 8, 299-310, 10.1046/j.1365-2443.2002.00634.x.

Myllymaki, H., Valanne, S., Ramet, M., 2014. The *Drosophila* Imd signaling pathway. J Immunol 192, 3455-3462, 10.4049/jimmunol.1303309.

Nakahara, Y., Matsumoto, H., Kanamori, Y., Kataoka, H., Mizoguchi, A., Kiuchi, M., Kamimura, M., 2006. Insulin signaling is involved in hematopoietic regulation in an insect hematopoietic organ. J Insect Physiol 52, 105-111, 10.1016/j.jinsphys.2005.09.009.

Nakhleh, J., El Moussawi, L., Osta, M.A., 2017. Chapter 3 - The melanization response in insect immunity, in Advances in Insect Physiology, Ligoxygakis, P. (Ed.). Academic Press, pp. 83-109.

Nappi, A.J., Christensen, B.M., 2005. Melanogenesis and associated cytotoxic reactions: Applications to insect innate immunity. Insect Biochem Mol Biol 35, 443-459, 10.1016/j.ibmb.2005.01.014.

Navarro-Cerrillo, G., Ferre, J., de Maagd, R.A., Herrero, S., 2012. Functional interactions between members of the REPAT family of insect pathogen-induced proteins. Insect Mol Biol 21, 335-342, 10.1111/j.1365-2583.2012.01139.x.

Navarro-Cerrillo, G., Hernandez-Martinez, P., Vogel, H., Ferre, J., Herrero, S., 2013. A new gene superfamily of pathogen-response (repat) genes in *Lepidoptera*: classification and expression analysis. Comp Biochem Physiol B-Biochem Physiol 164, 10-17, 10.1016/j.cbpb.2012.09.004.

Nazario-Toole, A.E., Wu, L.P., 2017. Phagocytosis in insect immunity, in Advances in Insect Physiology, Volume 52, Ligoxygakis, P. (Ed.). Kruze, K., pp. 35-73.

Ozakman, Y., Eleftherianos, I., 2019. TGF-β signaling interferes with the *Drosophila* innate immune and metabolic response to parasitic nematode infection. Front Physiol 10, 10.3389/Fphys.2019.00716.

Pace, K.E., Baum, L.G., 2002. Insect galectins: Roles in immunity and development. Glycoconjugate J 19, 607-614, 10.1023/B:Glyc.0000014092.86763.2f.

Park, Y., Herbert, E.E., Cowles, C.E., Cowles, K.N., Menard, M.L., Orchard, S.S., Goodrich-Blair, H., 2007. Clonal variation in *Xenorhabdus nematophila* virulence and suppression of *Manduca sexta* immunity. Cell Microbiol 9, 645-656, 10.1111/j.1462-5822.2006.00815.x.

Park, Y., Kim, Y., 2000. Eicosanoids rescue *Spodoptera exigua* infected with *Xenorhabdus nematophilus*, the symbiotic bacteria to the entomopathogenic nematode *Steinernema carpocapsae*. J Insect Physiol 46, 1469-1476, 10.1016/S0022-1910(00)00071-8.

Park, Y., Stanley, D., 2006. The entomopathogenic bacterium, *Xenorhabdus nematophila*, impairs hemocytic immunity by inhibition of eicosanoid biosynthesis in adult crickets, *Gryllus firmus*. Biol Control 38, 247-253, 10.1016/j.biocontrol.2005.11.002.

Pastor-Pareja, J.C., Wu, M., Xu, T., 2008. An innate immune response of blood cells to tumors and tissue damage in *Drosophila*. Dis Model Mech 1, 144-154, 10.1242/dmm.000950.

Patrnogic, J., Heryanto, C., Eleftherianos, I., 2018. Wounding-induced upregulation of the Bone Morphogenic Protein signaling pathway in *Drosophila* promotes survival against parasitic nematode infection. Gene 673, 112-118, 10.1016/j.gene.2018.06.052.

963 Pimentel, H., Bray, N.L., Puente, S., Melsted, P., Pachter, L., 2017. Differential analysis of RNA-seq incorporating
964 quantification uncertainty. Nat Methods 14, 687-690, 10.1038/nmeth.4324.
965 Poinar, G.O., Grewal, P.S., 2012. History of entomopathogenic nematology. J Nematol 44, 153-161.
966 Poitout, S., Buès, R., 1970. Elevage de plusieurs espèces de Lépidoptères Noctuidae sur milieu artificiel riche et
967 sur milieu artificiel simplifié. Ann Zool Ecol Anim 2, 79-91.
968 Qiao, C., Li, J., Wei, X.H., Wang, J.L., Wang, Y.F., Liu, X.S., 2014. SRP gene is required for *Helicoverpa armigera*
969 prophenoloxidase activation and nodulation response. Dev Comp Immunol 44, 94-99,
970 10.1016/j.dci.2013.11.016.
971 Qu, Z.P., Adelson, D.L., 2012. Identification and comparative analysis of ncRNAs in human, mouse and zebrafish
972 Indicate a conserved role in regulation of genes expressed in brain. PLoS One 7, e52275,
973 10.1371/journal.pone.0052275.
974 R Core Team, 2017. R: A language and environment for statistical computing. R Foundation for Statistical
975 Computing, Vienna, Austria, URL https://www.R-project.org/.
976 Ribeiro, C., Duvic, B., Oliveira, P., Givaudan, A., Palha, F., Simoes, N., Brehelin, M., 1999. Insect immunity - effects
977 of factors produced by a nematobacterial complex on immunocompetent cells. J Insect Physiol 45, 677-685,
978 10.1016/S0022-1910(99)00043-8.
979 Ribeiro, C., Vignes, M., Brehelin, M., 2003. *Xenorhabdus nematophila* (Enterobacteriacea) secretes a cation-
980 selective calcium-independent porin which causes vacuolation of the rough endoplasmic reticulum and cell
981 lysis. J Biol Chem 278, 3030-3039, 10.1074/jbc.M210353200.
982 Roote, C.E., Zusman, S., 1996. Alternatively spliced forms of the *Drosophila* αPS2 subunit of integrin are sufficient
983 for viability and can replace the function of the αPS1 subunit of integrin in the retina. Development 122,
984 1985-1994.
985 Rowley, A.F., Ratcliffe, N.A., 1978. Histological study of wound-healing and hemocyte function in wax moth
986 *Galleria mellonella*. J Morphol 157, 181-199, 10.1002/jmor.1051570206.
987 Satyavathi, V.V., Mohamed, A.A., Kumari, S., Mamatha, D.M., Duvic, B., 2018. The IMD pathway regulates
988 lysozyme-like proteins (LLPs) in the silkmoth *Antheraea mylitta*. J Invertebr Pathol 154, 102-108,
989 10.1016/j.jip.2018.04.006.
990 Schmucker, D., Taubert, H., Jackle, H., 1992. Formation of the *Drosophila* larval photoreceptor organ and its
991 neuronal differentiation require continuous Krüppel gene activity. Neuron 9, 1025-1039, 10.1016/0896-
992 6273(92)90063-J.
993 Shin, S.W., Park, S.S., Park, D.S., Kim, M.G., Kim, S.C., Brey, P.T., Park, H.Y., 1998. Isolation and characterization of
994 immune-related genes from the fall webworm, *Hyphantria cunea*, using PCR-based differential display and
995 subtractive cloning. Insect Biochem Mol Biol 28, 827-837.
996 Shokal, U., Eleftherianos, I., 2017. The *Drosophila* Thioester containing Protein-4 participates in the induction of
997 the cellular immune response to the pathogen *Photorhabdus*. Dev Comp Immunol 76, 200-208,
998 10.1016/j.dci.2017.06.008.
999 Shokal, U., Kopydlowski, H., Eleftherianos, I., 2017. The distinct function of Tep2 and Tep6 in the immune defense
1000 of *Drosophila melanogaster* against the pathogen *Photorhabdus*. Virulence 8, 1668-1682,
1001 10.1080/21505594.2017.1330240.
1002 Shokal, U., Kopydlowski, H., Harsh, S., Eleftherianos, I., 2018. Thioester-containing proteins 2 and 4 affect the
1003 metabolic activity and inflammation response in *Drosophila*. Infect Immun 86, 10.1128/IAI.00810-17.
1004 Sicard, M., Brugirard-Ricaud, K., Pages, S., Lanois, A., Boemare, N.E., Brehelin, M., Givaudan, A., 2004. Stages of
1005 infection during the tripartite interaction between *Xenorhabdus nematophila*, its nematode vector, and
1006 insect hosts. Appl Environ Microbiol 70, 6473-6480, 10.1128/AEM.70.11.6473-6480.2004.
1007 Sowa-Jasilek, A., Zdybicka-Barabas, A., Staczek, S., Wydrych, J., Mak, P., Jakubowicz, T., Cytrynska, M., 2014.
1008 Studies on the role of insect hemolymph polypeptides: *Galleria mellonella* anionic peptide 2 and lysozyme.
1009 Peptides 53, 194-201, 10.1016/j.peptides.2014.01.012.
1010 Stofanko, M., Kwon, S.Y., Badenhorst, P., 2008. A misexpression screen to identify regulators of *Drosophila* larval
1011 hemocyte development. Genetics 180, 253-267, 10.1534/genetics.108.089094.
1012 Strand, M.R., 2008. The insect cellular immune response. Insect Sci 15, 1-14, 10.1111/j.1744-7917.2008.00183.x.
1013 Stuart, L.M., Deng, J.S., Silver, J.M., Takahashi, K., Tseng, A.A., Hennessy, E.J., Ezekowitz, R.A.B., Moore, K.J., 2005.
1014 Response to *Staphylococcus aureus* requires CD36-mediated phagocytosis triggered by the COOH-terminal
1015 cytoplasmic domain. J Cell Biol 170, 477-485, 10.1083/jcb.200501113.

Tailliez, P., Pages, S., Ginibre, N., Boemare, N., 2006. New insight into diversity in the genus *Xenorhabdus*, including the description of ten novel species. Int J Syst Evol Microbiol 56, 2805-2818, 10.1099/ijs.0.64287-0.

Tang, H.P., 2009. Regulation and function of the melanization reaction in *Drosophila*. Fly 3, 105-111, 10.4161/Fly.3.1.7747.

Thurston, G.S., Yule, W.N., Dunphy, G.B., 1994. Explanations for the low susceptibility of *Leptinotarsa decemlineata* to *Steinernema carpocapsae*. Biol Control 4, 53-58, 10.1006/bcon.1994.1010.

Tingvall, T.O., Roos, E., Engstrom, Y., 2001. The Imd gene is required for local Cecropin expression in *Drosophila* barrier epithelia. EMBO Rep 2, 239-243.

Toubarro, D., Avila, M.M., Hao, Y.J., Balasubramanian, N., Jing, Y.J., Montiel, R., Faria, T.Q., Brito, R.M., Simoes, N., 2013a. A serpin released by an entomopathogen impairs clot formation in insect defense system. PLoS One 8, e69161, 10.1371/journal.pone.0069161.

Toubarro, D., Avila, M.M., Montiel, R., Simoes, N., 2013b. A pathogenic nematode targets recognition proteins to avoid insect defenses. PLoS One 8, e75691, 10.1371/journal.pone.0075691.

Tzou, P., Ohresser, S., Ferrandon, D., Capovilla, M., Reichhart, J.M., Lemaitre, B., Hoffmann, J.A., Imler, J.L., 2000. Tissue-specific inducible expression of antimicrobial peptide genes in *Drosophila* surface epithelia. Immunity 13, 737-748, 10.1016/S1074-7613(00)00072-8.

Untergasser, A., Cutcutache, I., Koressaar, T., Ye, J., Faircloth, B.C., Remm, M., Rozen, S.G., 2012. Primer3--new capabilities and interfaces. Nucleic Acids Res 40, e115, 10.1093/nar/gks596.

Urbano, J.M., Dominguez-Gimenez, P., Estrada, B., Martin-Bermudo, M.D., 2011. PS integrins and laminins: Key regulators of cell migration during *Drosophila* embryogenesis. PLoS One 6, e23893, 10.1371/journal.pone.0023893.

Valanne, S., Wang, J.H., Ramet, M., 2011. The *Drosophila* Toll Signaling Pathway. J Immunol 186, 649-656, 10.4049/jimmunol.1002302.

van Sambeek, J., Wiesner, A., 1999. Successful parasitation of locusts by entomopathogenic nematodes is correlated with inhibition of insect phagocytes. J Invertebr Pathol 73, 154-161, 10.1006/jipa.1998.4823.

Veillard, F., Troxler, L., Reichhart, J.M., 2016. *Drosophila melanogaster* clip-domain serine proteases: Structure, function and regulation. Biochimie 122, 255-269, 10.1016/j.biochi.2015.10.007.

Vertyporokh, L., Wojda, I., 2017. Expression of the insect metalloproteinase inhibitor IMPI in the fat body of *Galleria mellonella* exposed to infection with *Beauveria bassiana*. Acta Biochim Pol 64, 273-278, 10.18388/abp.2016_1376.

Vigneux, F., Zumbihl, R., Jubelin, G., Ribeiro, C., Poncet, J., Baghdiguian, S., Givaudan, A., Brehelin, M., 2007. The xaxAB genes encoding a new apoptotic toxin from the insect pathogen *Xenorhabdus nematophila* are present in plant and human pathogens. J Biol Chem 282, 9571-9580, 10.1074/jbc.M604301200.

Wang, Y., Branicky, R., Noe, A., Hekimi, S., 2018. Superoxide dismutases: Dual roles in controlling ROS damage and regulating ROS signaling. J Cell Biol 217, 1915-1928, 10.1083/jcb.201708007.

Wang, Y., Gaugler, R., Cui, L.W., 1994. Variations in immune response of *Popillia japonica* and *Acheta domesticus* to *Heterorhabditis bacteriophora* and *Steinernema* species. J Nematol 26, 11-18.

Wang, Z., Wilhelmsson, C., Hyrsl, P., Loof, T.G., Dobes, P., Klupp, M., Loseva, O., Morgelin, M., Ikle, J., Cripps, R.M., Herwald, H., Theopold, U., 2010. Pathogen entrapment by transglutaminase -- a conserved early innate immune mechanism. PLoS Pathog 6, e1000763, 10.1371/journal.ppat.1000763.

Wedde, M., Weise, C., Kopacek, P., Franke, P., Vilcinskas, A., 1998. Purification and characterization of an inducible metalloprotease inhibitor from the hemolymph of greater wax moth larvae, *Galleria mellonella*. Eur J Biochem 255, 535-543, 10.1046/j.1432-1327.1998.2550535.x.

Wedde, M., Weise, C., Nuck, R., Altincicek, B., Vilcinskas, A., 2007. The insect metalloproteinase inhibitor gene of the lepidopteran *Galleria mellonella* encodes two distinct inhibitors. Biol Chem 388, 119-127, 10.1515/Bc.2007.013.

White, G.F., 1927. A method for obtaining infective nematode larvae from cultures. Science 66, 302-303, 10.1126/science.66.1709.302-a.

Wu, S., Zhang, X.F., He, Y.Q., Shuai, J.B., Chen, X.M., Ling, E.J., 2010. Expression of antimicrobial peptide genes in *Bombyx mori* gut modulated by oral bacterial infection and development. Dev Comp Immunol 34, 1191-1198, 10.1016/j.dci.2010.06.013.

Xia, X., You, M., Rao, X.J., Yu, X.Q., 2018. Insect C-type lectins in innate immunity. Dev Comp Immunol 83, 70-79, 10.1016/j.dci.2017.11.020.

1070 Yadav, S., Daugherty, S., Shetty, A.C., Eleftherianos, I., 2017. RNAseq analysis of the *Drosophila* response to the
1071 entomopathogenic nematode *Steinernema*. G3 (Bethesda) 7, 1955-1967, 10.1534/g3.117.041004.
1072 Yadav, S., Eleftherianos, I., 2018. The Imaginal Disc Growth Factors 2 and 3 participate in the *Drosophila* response
1073 to nematode infection. Parasite Immunol 40, 10.1111/pim.12581.
1074 Yadav, S., Eleftherianos, I., 2019. Participation of the serine protease Jonah66Ci in the *Drosophila* antinematode
1075 immune response. Infect Immun 87, 10.1128/IAI.00094-19.
1076 Yadav, S., Gupta, S., Eleftherianos, I., 2018. Differential regulation of immune signaling and survival response in
1077 *Drosophila melanogaster* larvae upon *Steinernema carpocapsae* nematode infection. Insects 9,
1078 10.3390/Insects9010017.
1079 Yi, H.Y., Chowdhury, M., Huang, Y.D., Yu, X.Q., 2014. Insect antimicrobial peptides and their applications. Appl
1080 Microbiol Biotechnol 98, 5807-5822, 10.1007/s00253-014-5792-6.
1081 Yu, K.H., Kim, K.N., Lee, J.H., Lee, H.S., Kim, S.H., Cho, K.Y., Nam, M.H., Lee, I.H., 2002. Comparative study on
1082 characteristics of lysozymes from the hemolymph of three lepidopteran larvae, *Galleria mellonella*, *Bombyx*
1083 *mori*, *Agrius convolvuli*. Dev Comp Immunol 26, 707-713, 10.1016/S0145-305x(02)00027-7.
1084 Yu, X.Q., Kanost, M.R., 2004. Immulectin-2, a pattern recognition receptor that stimulates hemocyte
1085 encapsulation and melanization in the tobacco hornworm, *Manduca sexta*. Dev Comp Immunol 28, 891-
1086 900, 10.1016/j.dci.2004.02.005.
1087 Yuan, C.F., Xing, L.S., Wang, M.L., Wang, X., Yin, M.Y., Wang, Q.R., Hu, Z.H., Zou, Z., 2017. Inhibition of
1088 melanization by serpin-5 and serpin-9 promotes baculovirus infection in cotton bollworm *Helicoverpa*
1089 *armigera*. PLoS Pathog 13, e1006645, 10.1371/journal.ppat.1006645.
1090 Zhang, K., Pan, G.Z., Zhao, Y.Z., Hao, X.W., Li, C.Y., Shen, L., Zhang, R., Su, J.J., Cui, H.J., 2017. A novel immune-
1091 related gene HDD1 of silkworm *Bombyx mori* is involved in bacterial response. Mol Immunol 88, 106-115,
1092 10.1016/j.molimm.2017.06.023.
1093 Zhang, S., Yan, H., Li, C.Z., Chen, Y.H., Yuan, F.H., Chen, Y.G., Weng, S.P., He, J.G., 2013. Identification and function
1094 of leucine-rich repeat flightless-I-interacting protein 2 (LRRFIP2) in *Litopenaeus vannamei*. PLoS One 8,
1095 e57456, 10.1371/journal.pone.0057456.
1096 Zhuang, S.F., Kelo, L.S., Nardi, J.B., Kanost, M.R., 2007. An integrin-tetraspanin interaction required for cellular
1097 innate immune responses of an insect, *Manduca sexta*. J Biol Chem 282, 10.1074/Jbc.M700341200.
1098 Zou, F.M., Lee, K.S., Kim, B.Y., Kim, H.J., Gui, Z.Z., Zhang, G.Z., Guo, X.J., Jin, B.R., 2015. Differential and spatial
1099 regulation of the prophenoloxidase (proPO) and proPO-activating enzyme in cuticular melanization and
1100 innate immunity in *Bombyx mori* pupae. J Asia-Pac Entomol 18, 757-764, 10.1016/j.aspen.2015.09.007.
1101 Zou, Z., Shin, S.W., Alvarez, K.S., Kokoza, V., Raikhell, A.S., 2010. Distinct melanization pathways in the mosquito
1102 *Aedes aegypti*. Immunity 32, 41-53, 10.1016/j.immuni.2009.11.011.

1103

Figure Legends

Fig 1. Expression variations of the differentially expressed immune genes after infestation by the nematobacterial complex. Heatmaps showing the expression variations of the differentially expressed immune genes in the hemocytes and in the fat body at a middle time point of 15 h post-infestation. RNAseq raw data were retrieved from the study of Huot et al. (2019) in which three independent experiments were performed with N=9 larvae exposed to 150 NBCs or to a Ringer sterile solution in each sample. Differential expression between the infested and the control conditions was analyzed with the Sleuth software (following pseudoalignment with the Kallisto software) using statistical thresholds of 0.01 for q-value (equivalent of adjusted p-value), -1 and +1 for Beta value (biased equivalent of log2 fold change) and 5 for pseudocount means. The immune genes were identified by homology and classified as (A) antimicrobial immunity-related, (B) melanization-related, (C) cellular immunity-related and (D) diverse immune responses. Black dots indicate genes with statistically non-significant variations to the controls in the corresponding tissue; HC : Hemocytes, FB : Fat body.

Fig 2. Temporal dynamics of the identified immune responses after infestation by the nematobacterial complex. Heatmaps showing the temporal evolution of the induction levels of representative immune genes in the hemocytes (A) and in the fat body (B) after infestation by the NBC. Three independent experiments were performed with N=9 larvae exposed to 150 NBCs and N=9 larvae exposed to Ringer sterile solution. RT-qPCR experiments were performed in triplicate and the RpL32 housekeeping gene was used as reference for relative quantifications. Differential expression between the infested and the control conditions was assessed according to the method of Ganger et al. (2017) and with Student t tests on ΔCq. Black dots indicate genes with statistically non-significant variations to the controls in the corresponding tissue (p-value > 0.05). The dendrograms represent clustering analyses based on Pearson correlation coefficients.

Fig 3. Relative participations of *S. carpocapsae* and *X. nematophila* in the hemocytes' immune responses. Histograms showing the induction levels (+/- SEM) of representative immune genes in the hemocytes at 13 h after independent injections of either whole NBCs, axenic nematodes or bacterial symbionts. Three independent experiments were performed with N=9 control larvae and N=9 larvae injected with 10 NBCs (NBC), 10 axenic *S. carpocapsae* (*S.c.*) or 200 *X. nematophila* (*X.n.*). For NBC and axenic nematode injections control larvae were injected with 70 % Ringer - 30 % glycerol sterile solutions whereas they were injected with sterile PBS for bacterial injections. RT-qPCR experiments were performed in triplicate and the RpL32 housekeeping gene was used as reference for relative quantifications. Differential expression values between the infected and the corresponding control conditions were calculated according to the method of Ganger et al. (2017) and statistical differences between the three types of infection were assessed by one-way ANOVA and Tukey tests on ΔΔCq. Letters indicate the statistical groups resulting from the Tukey tests (p-value > 0.05). The genes were then gathered by type of immune

response with (A) antimicrobial immunity-related, (B) melanization-related, (C) cellular immunity-related and (D) diverse immune responses.

Fig 4. Relative participations of *S. carpocapsae* and *X. nematophila* in the fat body's immune responses. Histograms showing the induction levels (+/- SEM) of representative immune genes in the fat body at 13 h after independent injections of either whole NBCs, axenic nematodes or bacterial symbionts. Three independent experiments were performed with N=9 control larvae and N=9 larvae injected with 10 NBCs (NBC), 10 axenic *S. carpocapsae* (*S.c.*) or 200 *X. nematophila* (*X.n.*). For NBC and axenic nematode injections control larvae were injected with 70 % Ringer - 30 % glycerol sterile solutions whereas they were injected with sterile PBS for bacterial injections. RT-qPCR experiments were performed in triplicate and the RpL32 housekeeping gene was used as reference for relative quantifications. Differential expression values between the infected and the corresponding control conditions were calculated according to the method of Ganger et al. (2017) and statistical differences between the three types of infection were assessed by one-way ANOVA and Tukey tests on ΔΔCq. Letters indicate the statistical groups resulting from the Tukey tests (p-value > 0.05). The genes were then gathered by type of immune response with (A) antimicrobial immunity-related, (B) melanization-related and (C) diverse immune responses.

Fig 5. Transcriptional induction patterns of putative new immune genes. (A, C) Histograms showing the induction levels (+/- SEM) of 2 GBH genes in the hemocytes (A) and of the 5 Unk genes in the fat body (C) at several times after infestation by the NBC. Three independent experiments were performed with N=9 larvae exposed to 150 NBCs and N=9 larvae exposed to Ringer sterile solution. RT-qPCR experiments were performed in triplicate and the RpL32 housekeeping gene was used as reference for relative quantifications. Differential expression between the infested and the control conditions was assessed according to the method of Ganger et al. (2017) and with Student t tests on ΔCq. Black dots indicate genes with statistically non-significant variations to the controls (p-value > 0.05). (B, D) Histograms showing the induction levels (+/-SEM) of 2 GBH genes in the hemocytes (B) and of the 5 Unk genes in the fat body (D) at 13 h after independent injections of either whole NBCs, axenic nematodes or bacterial symbionts. Three independent experiments were performed with N=9 control larvae and N=9 larvae injected with 10 NBCs (NBC), 10 axenic *S. carpocapsae* (*S.c.*) or 200 *X. nematophila* (*X.n.*). For NBC and axenic nematode injections control larvae were injected with 70 % Ringer - 30 % glycerol sterile solutions whereas they were injected with sterile PBS for bacterial injections. RT-qPCR experiments were performed in triplicate and the RpL32 housekeeping gene was used as reference for relative quantifications. Differential expression values between the infected and the corresponding control conditions were calculated according to the method of Ganger et al. (2017) and statistical differences between the three types of infection were assessed by one-way ANOVA and Tukey tests on ΔΔCq. Letters indicate the statistical groups resulting from the Tukey tests (p-value > 0.05).

Fig 6. Hypothetical structure of the *S. frugiperda* larva's immune response to the NBC. Graphical abstract illustrating the main hypotheses we can emit from the present RNAseq and RT-qPCR data and from our current knowledge of *S. frugiperda* immunity. Dark green letters, lines and arrows indicate responses that seem to be mainly induced by the nematode partner *S. carpocapsae* whereas orange ones indicate responses that seem to be mainly induced by the bacterial symbiont *X. nematophila*. The arrows' thicknesses and the letter sizes refer to the relative strengths of the induced transcriptional responses.

Supporting Information Legends

Supplementary Table 1. Primers sequences and genes used in this study.

Supplementary Table 2. Hemocytes and fat body RNAseq results for *S. frugiperda*'s immune genes. RNAseq raw data were retrieved from the study of Huot et al. (2019) in which three independent experiments were performed with N=9 larvae exposed to 150 NBCs or to a Ringer sterile solution for 15 hours. Following pseudoalignment with the Kallisto software, differential expression between the infested and the control conditions was analyzed with the Sleuth software using statistical thresholds of 0.01 for q-value (equivalent of adjusted p-value), -1 and +1 for Beta value (biased equivalent of log2 fold change) and 5 for pseudocount means. The statistics corresponding to the transcripts that were considered as significantly up- or down-regulated are highlighted in red and blue, respectively. The normalized pseudocounts are also indicated for each individual sample, with HCn15 and FBn15 corresponding to control larvae and HCi15 and FBi15 corresponding to infested larvae. Blast hits on the *Drosophila* and nr NCBI databases were obtained by blastx with the Blast2GO software. (A) Immune genes previously annotated in the *S. frugiperda*'s genome. (B) Newly identified *S. frugiperda*'s immune genes.

Supplementary Table 3. Hemocytes and fat body RNAseq results for the Unk and GBH putative new immune genes. RNAseq raw data were retrieved from the study of Huot et al. (2019) in which three independent experiments were performed with N=9 larvae exposed to 150 NBCs or to a Ringer sterile solution for 15 hours. Following pseudoalignment with the Kallisto software, differential expression between the infested and the control conditions was analyzed with the Sleuth software using statistical thresholds of 0.01 for q-value (equivalent of adjusted p-value), -1 and +1 for Beta value (biased equivalent of log2 fold change) and 5 for pseudocount means. The statistics corresponding to the transcripts that were considered as significantly upregulated are highlighted in red. The normalized pseudocounts are also indicated for each individual sample, with HCn15 and FBn15 corresponding to control larvae and HCi15 and FBi15 corresponding to infested larvae.

Supplementary Fig 1. Verification of *S. carpocapsae* axenicity. Electrophoresis gel showing the absence of bacterial contaminants in the axenized nematodes used for experimental infections. Total DNA from ground infective stage nematodes was extracted a few hours after each experimental infection (fresh axenic *S.c.*) and after several days of storage without antibiotics (stored axenic *S.c.*). The absence of bacterial contaminations was assessed by agarose gel electrophoresis after PCR amplification of the 16S rRNA gene with universal primers and of the *Xenorhabdus*-specific XNC1_0073 gene (encoding a putative TonB-dependent heme-receptor). Whole NBCs (NBC) and a pure suspension of *X. nematophila* (*X.n.*) were used as positive controls. A pure suspension of *Pseudomonas protegens* (*P.p.*) was used as negative control of putative TonB-dependent heme-receptor amplification. The results indicate no bacterial contamination is detected in the sterile axenic nematodes used for experimental infections and

that even after several days of storage without antibiotics, the *X. nematophila* population did not recover within these nematodes.

Supplementary Fig 2. Temporal monitoring of nematobacterial infestation parameters. (A) Dotplot showing the number of *S. carpocapsae* nematodes detected in the midgut alimentary bolus at several times after contact with 150 NBCs. Dot colors correspond to 3 independent experiments on N=3 larvae per time point. (B) Curve showing the temporal evolution of *X. nematophila* concentration (+/-SEM) in the hemolymph across the time post-infestation. Three independent infestation experiments were performed with 3 pools of 3 larvae per time point. Hemolymph was collected by bleeding and *X. nematophila* was quantified by CFU counting on selective culture medium containing erythromycin. (C) Curve showing the temporal evolution of *S. frugiperda* larvae survival percentage (+/- SEM) across the time post-infestation. Three independent infestation experiments were performed on N=20 larvae per experiment.

Supplementary Fig 3. Comparison of the main infection parameters after independent injections of the nematobacterial complex, of axenic *S. carpocapsae* and of *X. nematophila*. (A) Curves showing the temporal evolution of *X. nematophila* concentration (+/-SEM) after independent injections of either 10 NBCs or 200 *X. nematophila* (*X.n.*). Three independent injection experiments were performed with 3 pools of 3 larvae per time point. Hemolymph was collected by bleeding and *X. nematophila* was quantified by CFU counting on selective culture medium containing erythromycin. (B) Curves showing the temporal evolution of *S. frugiperda* larvae survival percentage (+/- SEM) after independent injections of either 10 NBCs , 10 axenic *S. carpocapsae* (*S.c.*) or 200 *X. nematophila* (*X.n.*). Three independent injection experiments were performed on N=20 larvae per experiment. No insect death was reported for control buffer-injected larvae. (C) Histogram showing the parasitic success (+/- SEM) (i.e.: number of larvae with NBC emergence on total number of infested larvae) after independent injections of either 10 NBCs or 10 axenic *S. carpocapsae* (*S.c.*). Three independent injection experiments were performed on N=20 larvae per infection type and per experiment.

Supplementary Fig 4. Alignment of deduced amino acid sequences of Unks from *S. frugiperda* with those of *S. litura* and *S. littoralis*. Nucleotide sequences were retrieved by blastn on *S. litura* and *S. littoralis* genomes.

Figure 1

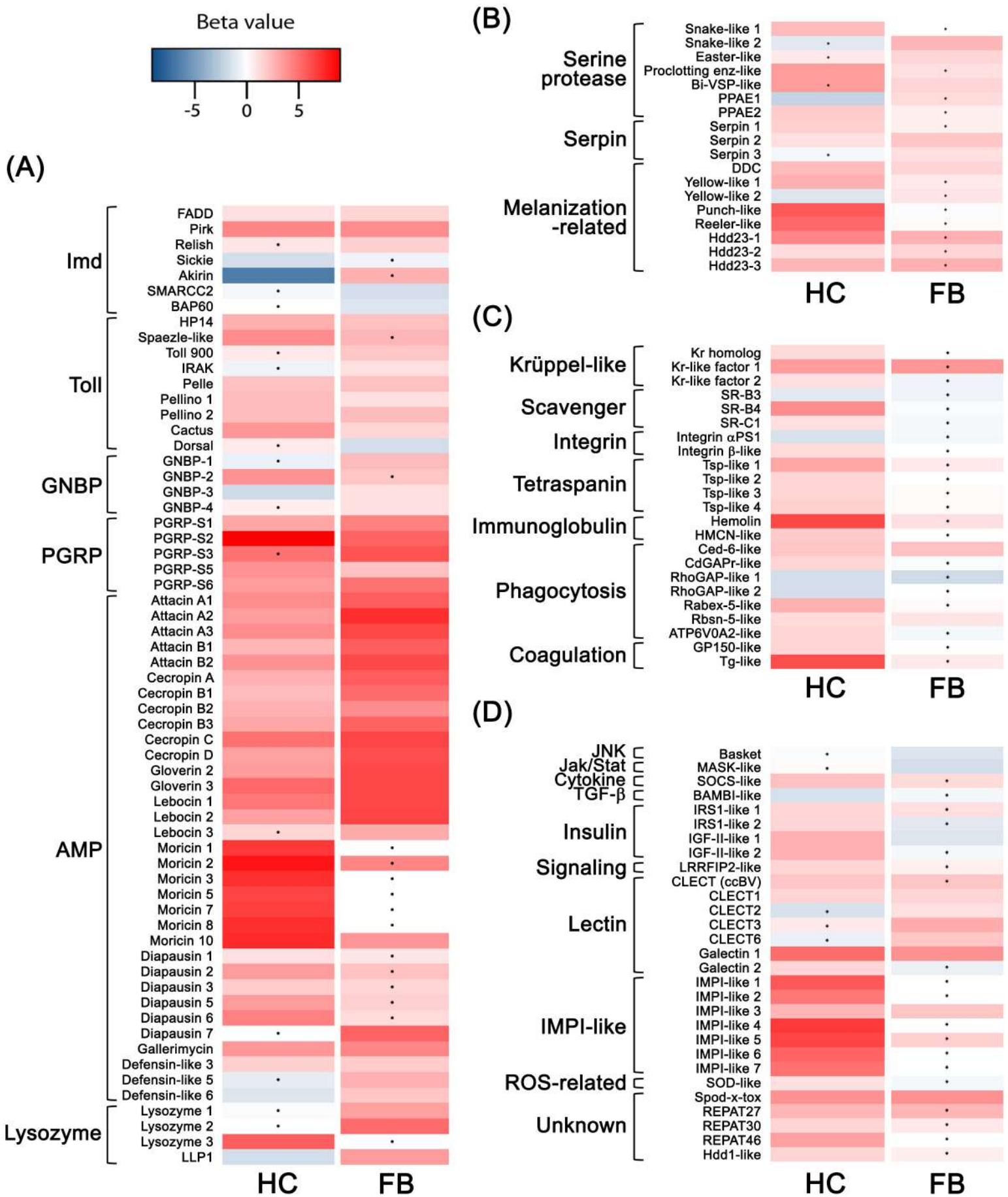
Beta value
-5
0
5
(A)
Imd
FADD
Pirk
Relish
Sickie
Akirin
SMARCC2
BAP60
Toll
HP14
Spaezle-like
Toll 900
IRAK
Pelle
Pellino 1
Pellino 2
Cactus
Dorsal
GNBP
GNBP-1
GNBP-2
GNBP-3
GNBP-4
PGRP
PGRP-S1
PGRP-S2
PGRP-S3
PGRP-S5
PGRP-S6
AMP
Attacin A1
Attacin A2
Attacin A3
Attacin B1
Attacin B2
Cecropin A
Cecropin B1
Cecropin B2
Cecropin B3
Cecropin C
Cecropin D
Gloverin 2
Gloverin 3
Lebocin 1
Lebocin 2
Lebocin 3
Moricin 1
Moricin 2
Moricin 3
Moricin 5
Moricin 7
Moricin 8
Moricin 10
Diapausin 1
Diapausin 2
Diapausin 3
Diapausin 5
Diapausin 6
Diapausin 7
Gallerimycin
Defensin-like 3
Defensin-like 5
Defensin-like 6
Lysozyme
Lysozyme 1
Lysozyme 2
Lysozyme 3
LLP1
HC
FB
(B)
Serine protease
Snake-like 1
Snake-like 2
Easter-like
Proclotting enz-like
Bi-VSP-like
PPAE1
PPAE2
Serpin
Serpin 1
Serpin 2
Serpin 3
Melanization -related
DDC
Yellow-like 1
Yellow-like 2
Punch-like
Reeler-like
Hdd23-1
Hdd23-2
Hdd23-3
HC
FB
(C)
Krüppel-like
Kr homolog
Kr-like factor 1
Kr-like factor 2
Scavenger
SR-B3
SR-B4
SR-C1
Integrin
Integrin αPS1
Integrin β-like
Tetraspanin
Tsp-like 1
Tsp-like 2
Tsp-like 3
Tsp-like 4
Immunoglobulin
Hemolin
HMCN-like
Phagocytosis
Ced-6-like
CdGAPr-like
RhoGAP-like 1
RhoGAP-like 2
Rabex-5-like
Rbsn-5-like
ATP6V0A2-like
Coagulation
GP150-like
Tg-like
HC
FB
(D)
JNK
Jak/Stat
Cytokine
TGF-β
Basket
MASK-like
SOCS-like
BAMBI-like
Insulin
IRS1-like 1
IRS1-like 2
IGF-II-like 1
IGF-II-like 2
Signaling
LRRFIP2-like
Lectin
CLECT (ccBV)
CLECT1
CLECT2
CLECT3
CLECT6
Galectin 1
Galectin 2
IMPI-like
IMPI-like 1
IMPI-like 2
IMPI-like 3
IMPI-like 4
IMPI-like 5
IMPI-like 6
IMPI-like 7
ROS-related
SOD-like
Unknown
Spod-x-tox
REPAT27
REPAT30
REPAT46
Hdd1-like
HC
FB

Figure 2

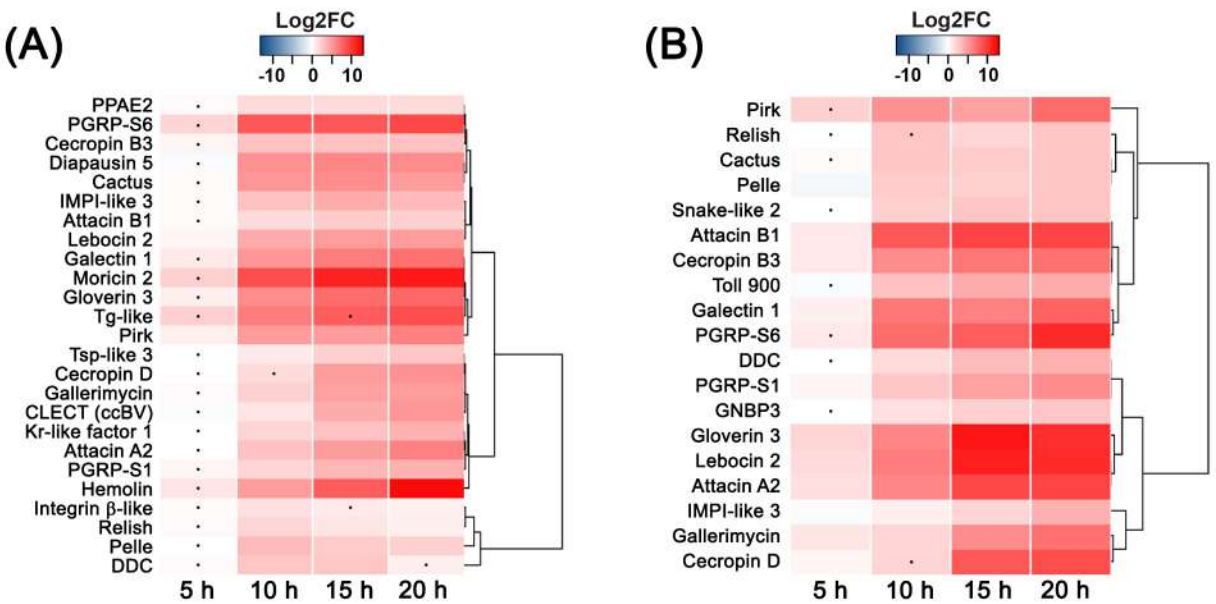
(A)
Log2FC
-10 0 10
PPAE2
PGRP-S6
Cecropin B3
Diapausin 5
Cactus
IMPI-like 3
Attacin B1
Lebocin 2
Galectin 1
Moricin 2
Gloverin 3
Tg-like
Pirk
Tsp-like 3
Cecropin D
Gallerimycin
CLECT (ccBV)
Kr-like factor 1
Attacin A2
PGRP-S1
Hemolin
Integrin β-like
Relish
Pelle
DDC
5 h
10 h
15 h
20 h
(B)
Log2FC
-10 0 10
Pirk
Relish
Cactus
Pelle
Snake-like 2
Attacin B1
Cecropin B3
Toll 900
Galectin 1
PGRP-S6
DDC
PGRP-S1
GNBP3
Gloverin 3
Lebocin 2
Attacin A2
IMPI-like 3
Gallerimycin
Cecropin D
5 h
10 h
15 h
20 h

Figure 3

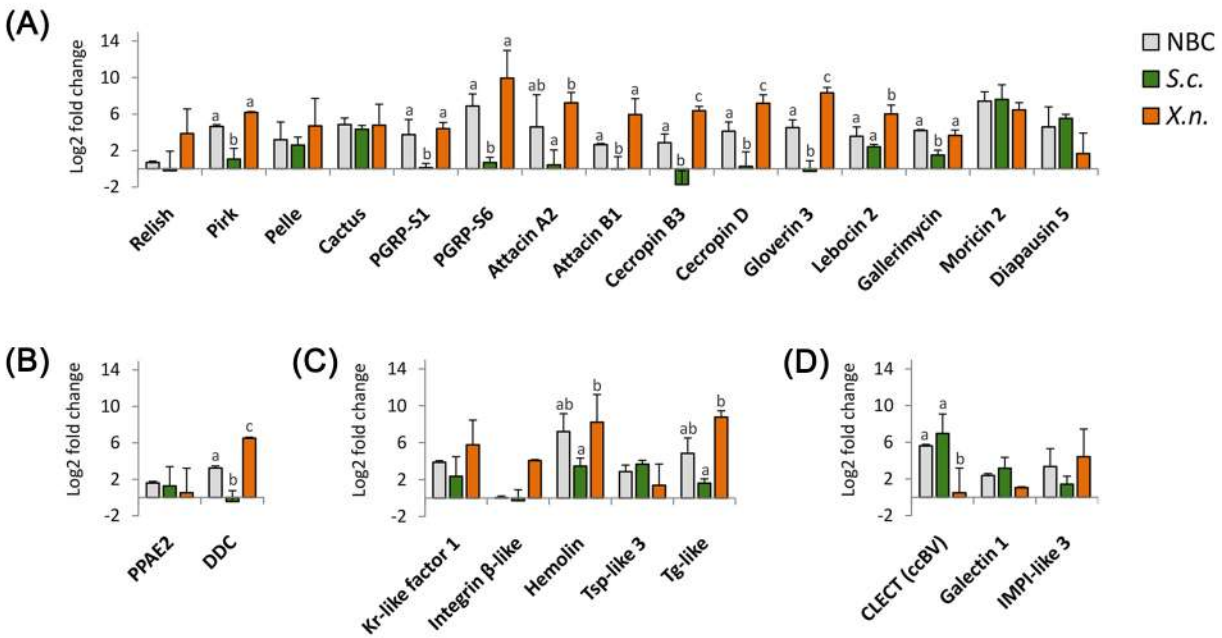
(A)
Log2 fold change
14
10
6
2
-2
NBC
S.c.
X.n.
Relish
Pirk
Pelle
Cactus
PGRP-S1
PGRP-S6
Attacin A2
Attacin B1
Cecropin B3
Cecropin D
Gloverin 3
Lebocin 2
Gallerimycin
Moricin 2
Diapausin 5
(B)
PPAE2
DDC
(C)
Kr-like factor 1
Integrin β-like
Hemolin
Tsp-like 3
Tg-like
(D)
CLECT (ccBV)
Galectin 1
IMPI-like 3

Figure 4

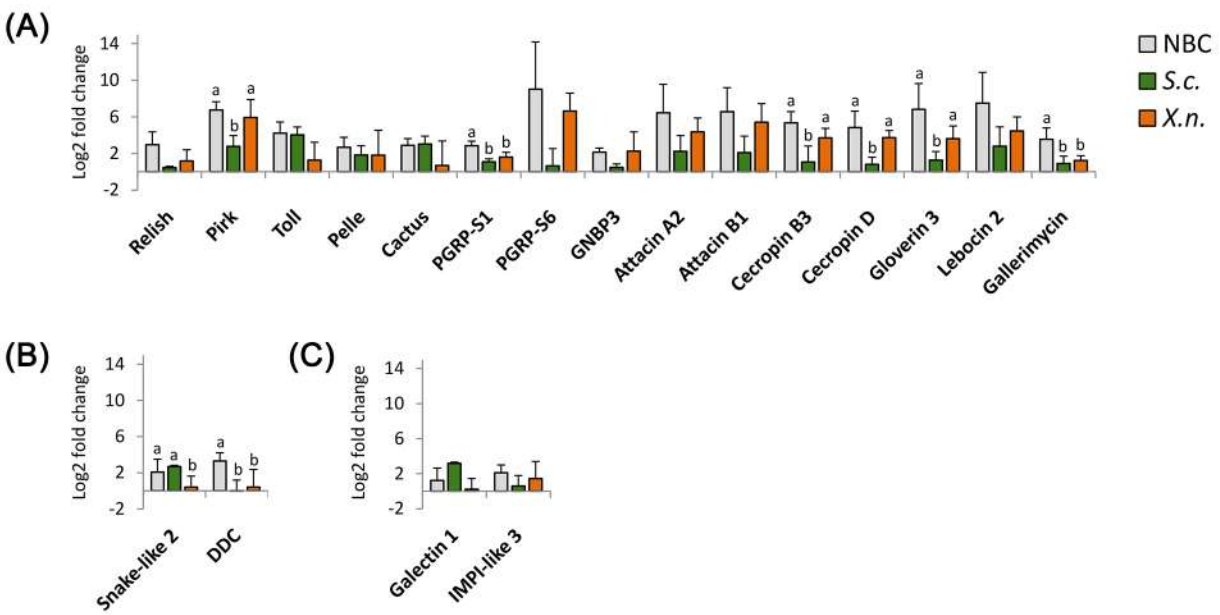
(A)
Log2 fold change
14
10
6
2
-2
NBC
S.c.
X.n.
Relish
Pirk
Toll
Pelle
Cactus
PGRP-S1
PGRP-S6
GNBP3
Attacin A2
Attacin B1
Cecropin B3
Cecropin D
Gloverin 3
Lebocin 2
Gallerimycin
(B)
Snake-like 2
DDC
(C)
Galectin 1
IMPI-like 3

Figure 5

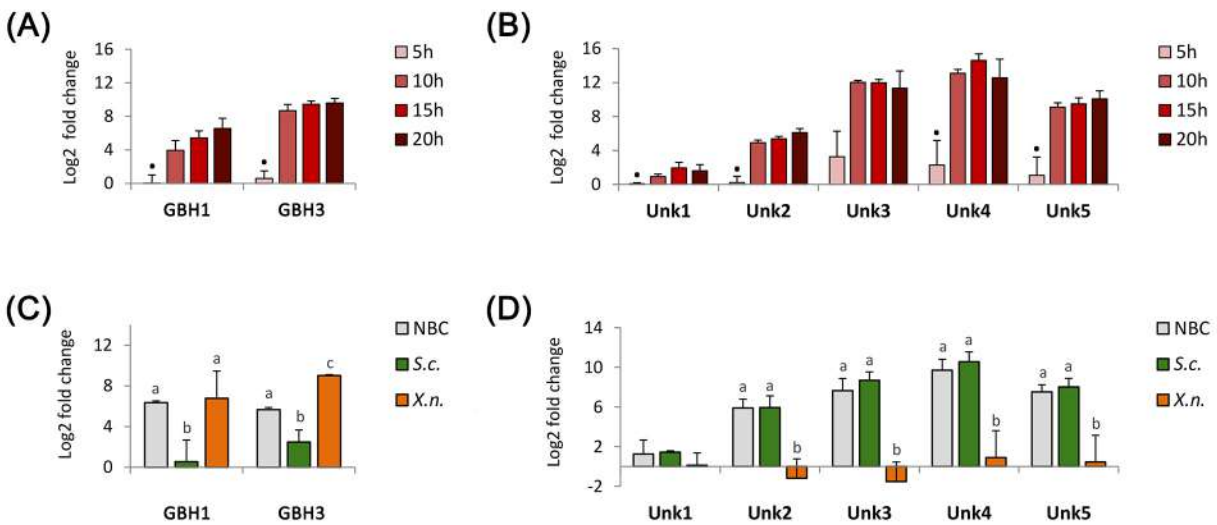
(A)
Log2 fold change
16
12
8
4
0
GBH1
GBH3
5h
10h
15h
20h
(B)
Log2 fold change
16
12
8
4
0
Unk1
Unk2
Unk3
Unk4
Unk5
5h
10h
15h
20h
(C)
Log2 fold change
12
8
4
0
a
b
a
a
b
c
GBH1
GBH3
NBC
S.c.
X.n.
(D)
Log2 fold change
14
10
6
2
-2
a
a
b
a
a
b
a
a
b
a
a
b
Unk1
Unk2
Unk3
Unk4
Unk5
NBC
S.c.
X.n.

Figure 6

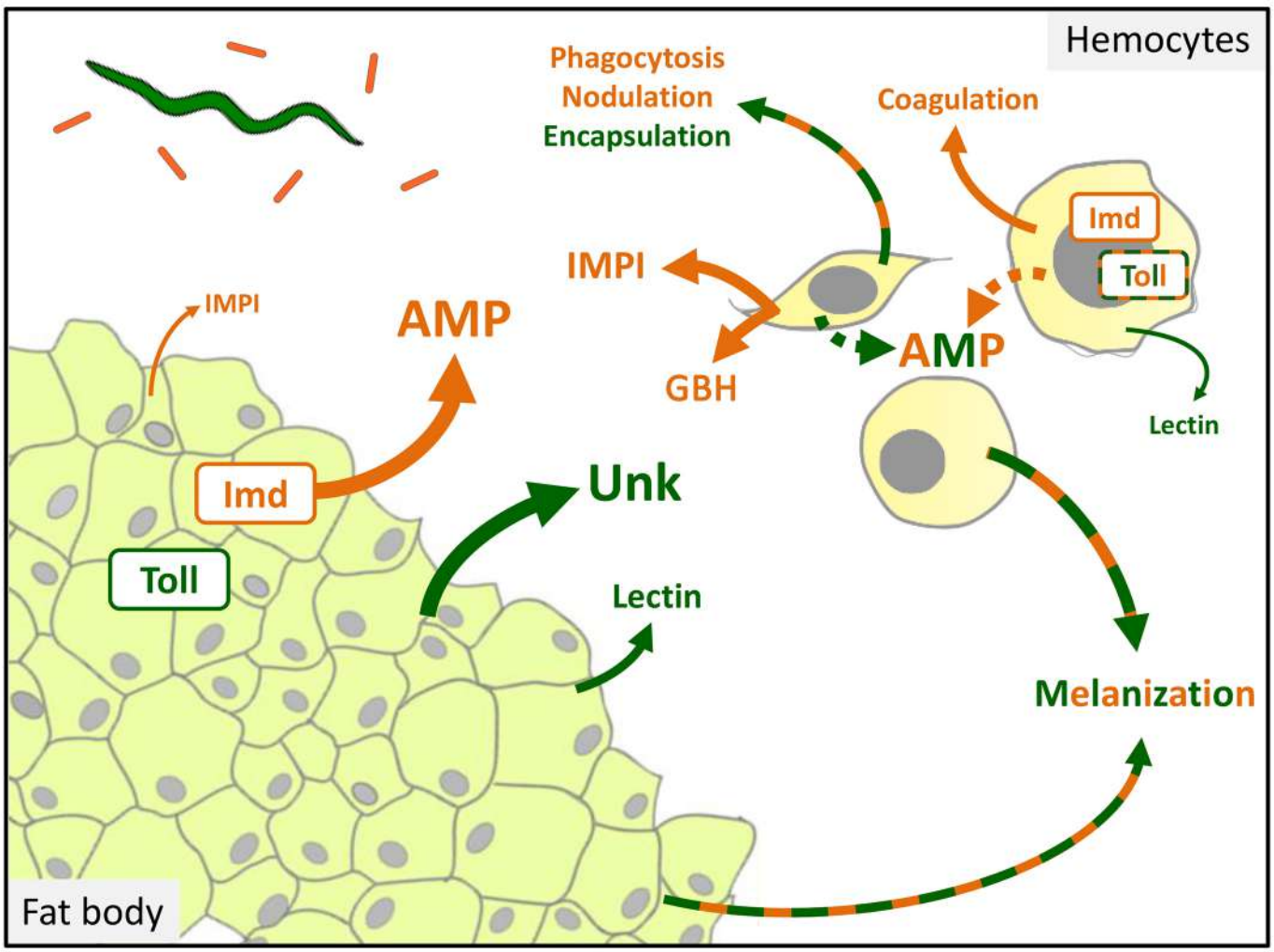
Hemocytes
Phagocytosis
Nodulation
Encapsulation
Coagulation
Imd
Toll
IMPI
GBH
AMP
Lectin
IMPI
AMP
Imd
Toll
Unk
Lectin
Melanization
Fat body